HORIZON 2020

HORIZON 2020 RESEARCH AND INNOVATION FRAMEWORK PROGRAMME OF THE EUROPEAN ATOMIC ENERGY COMMUNITY

Nuclear Fission and Radiation Protection 2018 (NFRP-2018-4)

Project acronym:	**SANDA**
Project full title:	**Solving Challenges in Nuclear Data for the Safety of European Nuclear facilities**
Grant Agreement no.:	**H2020 Grant Agreement number: 847552**

Workpackage N°:	***WP4***
Identification N°:	***D4.6***
Type of document:	***Deliverable***
Title:	REPORT ON THE APPLICATIONS: RECOMMENDATION
Dissemination Level:	***PU***
Reference:	
Status:	***VERSION 1***
Comments:	….

	Name	Partner	Date	Signature
Prepared by:	V. Bécares			Firmado por BECARES PALACIOS VICENTE -
WP leader:	D. A. Rochman			
IP Co-ordinator:	E. González			

Signed by GONZALEZ ROMERO ENRIQUE MIGUEL - DNI ***3708** 25/05/2023 with a certificate emitted by AC Sector Público

SANDA Project D4.6: Report on the applications: recommendation

V. Bécares[1], J. Llanes-Gamonoso[1], S. Panizo[1], A. Sánchez-Caballero[1], D. Álvarez-Fernández[1], G. Žerovnik[2], O. Cabellos[3], I. Kodeli[4], G. Letnar[5]

[1]*CIEMAT, Avenida Complutense, 40, 28040 Madrid (Spain).*

[2]*Jožef Stefan Institute, Jamova cesta 39, 1000 Ljubljana (Slovenia).*

[3]*Universidad Politécnica de Madrid (UPM), José Gutiérrez Abascal, 2, 28006 Madrid (Spain).*

[4]*UKAEA, Culham Centre for Fusion Energy, Abingdon, OX14 3DB, UK*

[5]*Faculty of Mathematics and Physics, University of Ljubljana, Jadranska ulica 19, 1000 Ljubljana (Slovenia).*

** Current address: SCK CEN, Boeretang 200, 2400 Mol (Belgium).*

Contact: vicente.becares@ciemat.es, Tel: +34 91 346 63 85.

Contents

1. Introduction

Horizon 2020 SANDA project aims to coordinate all European activities regarding nuclear data, including experimental measurements (work packages 1, 2 and 3), evaluation (work package 4) and validation (work package 5), with the particular aim to contribute to the development of the future JEFF-4 nuclear data library.

Within WP4, focused on evaluation and uncertainties, a task has been included (task 4.4) whose objective is recommending a series of benchmark experiments for the validation of new nuclear data evaluations. More specifically, the description of this task reads:

> *"To complete this work package and provide a suitable link with the Work Package on validation (WP5), recommendations for preferred benchmark for thermal and high energy (up to 20 MeV) will be proposed. Whereas nuclear data validation has been in the recent years mostly restricted to critical benchmarks, this effort will also focus on other types of measurements, such as shielding benchmarks and kinetics. The code such as SUS3D (JSI) will be used for shielding calculations, with improved S/U analysis of the impact of the uncertainties in the secondary angular and energy distributions. For criticality and kinetic parameters, a review of different suites of inputs used in ICSBEP will be performed (CIEMAT and UPM), with selection/classification of benchmarks for different levels of nuclear data sensitivities for benchmarking and validation of nuclear data. For shielding, and spent nuclear fuel, a review of the SINBAD and SFCOMPO databases will be performed (JSI)"*

This report intends to fulfil these requirements. It is organized in four major sections, one for every type of benchmarks considered:

- ***Section 2: criticality benchmarks***. In this section, recommendations about the procedures to follow to select adequate sets of benchmarks for validation of specific nuclear data are presented, based on the work performed within the JEFF Working Group on Benchmarking, alongside with some specific examples.
- ***Section 3: shielding benchmarks***. This section presents an overview of the current status of the SINBAD database, including the new formats introduced adopted in the ICSBEP/IRPhE meeting in 2019, and the most recent quality evaluations and benchmark analyses.
- ***Section 4: kinetic parameter benchmarks***. This includes both the effective delayed neutron fraction (β_{eff}) and the mean neutron generation time (Λ_{eff}). In OECD'/NEA's IRPhE reactor physics experiments database, experimental kinetic parameter information is available only for very few systems. Hence, additional information has been searched in the literature and is presented in Annex 1.
- ***Section 5: fuel burnup benchmarks***. In this section, an overview of OECD/NEA's SFCOMPO database is presented, as well as the results of some analysis performed by the institutions participating in this task (JSI, UPM).

2. Criticality benchmarks

The Quality & Assurance (Q&A) for the evaluated of nuclear reaction data files is performed against available internationally evaluated integral benchmark experiments. These "integral tests" or "benchmarks" are performed to systematically address both the performance of individual evaluations and the full nuclear data library.

Typically, the first benchmarking in criticality is carried out with ICSBEP [ICSBEP 2009] selecting "benchmarks" as simple single-physics experiments of non-trivial but well understood "clean" nuclear systems. It allows us to identify the real impact of nuclear data in the criticality integral experiments.

In this context, theJEFF Working Group on Benchmarking was stablished in 2022 [JEFF-Validation, 2022] within the JEFF project to provide steps for the validation of nuclear data libraries in the framework of JEFF-4.A summary of the main conclusions elaborated by this WG where the UPM has actively participated is presented below:

A total of seven steps were identified by this Working Group:

1. *Selection of representative criticality cases.*
2. *Upload the corresponding input decks (e.g. MCNP…) in a dedicated directory on GitLab.*
3. *Calculate the k_{eff} using different codes and data libraires.*
4. *Upload k_{eff} results in a dedicated results' directory on Gitlab.*
5. *Automated calculation of different Figure of Merit allowing to compare libraries.*
6. *Use of the NDAST tool to propagate the uncertainty associated with the nuclide cross sections to k_{eff}. Using the sensitivity values included in ICSBEP-DICE/NEA.*
7. *For each nuclide to be tested, use of a Generalized Linear Least Squares Methodology (GLLSM) tool in order to investigate the improvement needed in the nuclear data using integral experiments. Use of the sensitivity values collected by NEA from different partners and Institutions covering different nuclear reactor systems. Examples of such sensitivity profiles can be the ones distributed in D5.2 on "Report on ESFR, MYRRHA, and ALFRED sensitivity and impact studies" [Romojaro 2022].*

In addition, the Working Group concluded that the selection of representative criticality benchmarks should be done according to the following criteria:

- *For the selected criticality benchmarks, their experimental uncertainties should be evaluated correctly, and that they should be sufficiently low. It is therefore proposed to discard all experiments with propagated uncertainties in k_{eff} higher than 0.00500 at the 1σ level and lower than 0.00100 at the 1σ level.*
- *Specific benchmarks should be selected for testing specific target isotopes (e.g. iron) or specific energy regions (e.g unresolved resonance range (URR)) that are often encountered in criticality-safety, reactor physics, shielding and depletion calculations.*
- *"Benchmark suites" should not be restricted to only keff values, the effort is also focus on other types of measurements, such as reaction rates and kinetic parameters (e.g. βeff)..*
- *The selection of criticality experiments should be based on a sensitivity analysis performed with DICE/ICSBEP Handbook.*
- *High sensitivity to the nuclear data to be tested will be chosen as priority. The selection/classification of benchmarks with different levels of nuclear data sensitivities will help in the benchmarking and validation of nuclear data*
- *Testing should consider the whole energy range*

Therefore, this report contains four different suites of Benchmarks identified for nuclear data validation in criticality scenarios:

- A review of 123 Mosteller's suite.
- Iron-Benchmarking suite.
- Benchmark suite for testing the URR.
- Low-enriched Compound Thermal (LCTs) benchmarks for Criticality Safety Analysis (CSA) of PWR spent fuel pool and storage cask.

2.1. The "123-Mosteller's suite".

An expanded Criticality Validation Suite, taken from Integral Benchmark Experiments, ICSBEP for Criticality Safety containing 119 cases was proposed by R. D. Mosteller *et al.* [Mosteller 2005, LA-UR-11-05076] for a variety of fuels: plutonium (36), highly-enriched uranium (40), intermediate-enriched uranium (17), low-enriched uranium (8) and U-233 (18). For each type of fuel, there are cases with a variety of moderators, reflectors, spectra and geometries.

In addition, 4 cases also included in ICSBEP [ICSBEP 2009] are used for testing purposes: Np-237 (SPEC-META-FAST-008, Heavy-Water solutions (HEU-SOL-THERM-004-001), Very thermal Pu solution (PU-SOL-THERM-009) and Unmoderated ZEUS benchmark (HEU-MET-FAST-073). Appendix 2 in [UPM report: 2022-12-20/WP4-D4.6/R6] gives a short description of the 123-Mosteller's Benchmark suite used for benchmarking and testing nuclear data in criticality calculations. Examples of this benchmark suite can be found in the [JEFF-3.3 2018].

The reduced chi-square figure of merit allows an easy comparison of the performance of different nuclear data evaluations.

$$\chi^2/N = \sum_{i=1}^{N} \frac{(k_{C,i} - k_{E,i})^2}{\Delta k_{C,i}^2 + \Delta k_{E,i}^2}$$

where:

- N is the number of benchmarks.
- $k_{C,i}$ is the computed neutron multiplication factor for the i^{th}-benchmark using a particular computer code and a nuclear data library.
- $\Delta k_{C,i}^2$ is the statistical uncertainty in the calculation.
- $k_{E,i}$ is the experimental neutron multiplication factor for the i^{th}-benchmark model.
- $\Delta k_{E,i}^2$ is the experimental uncertainty of the evaluated i^{th}-benchmark model.

Then, χ^2/N value is a function of the overall performance of the "code + nuclear data library" for the overall set Benchmarks. If $\chi^2/N < 1$, on average, calculations match benchmarks to within one experimental plus statistical (Monte Carlo) uncertainty.

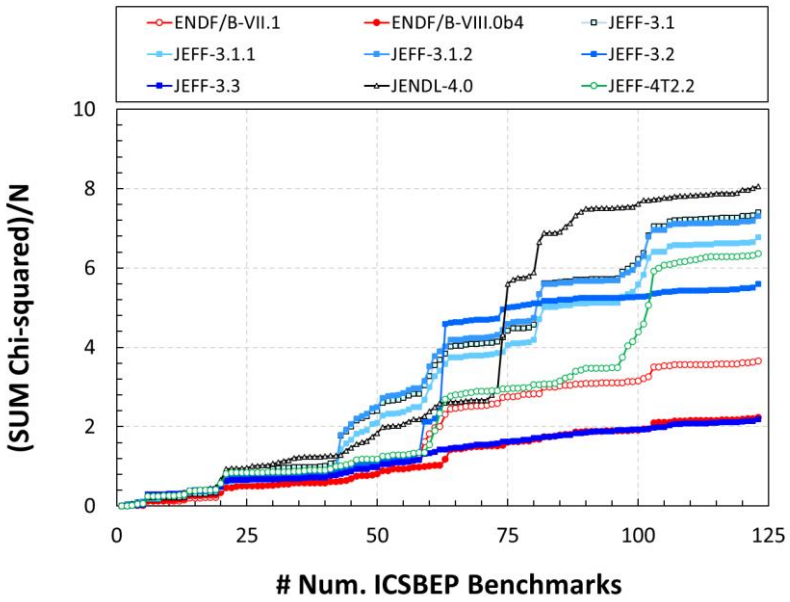

Figure 1. Comparison of cumulative chi-2 values using 123-Mosteller's suite

As an example, the cumulative plot (Figure 1) shows the improvements in new evaluations. For JEFF-3.3 with a rather good cumulative χ^2/N = 2.19. However, for the JEFF-4T2.2 released in March 2023 the performance is deteriorated and additional efforts for a final JEFF-4 evaluation are required to improve it.

2.2. Selection of criticality Benchmarks within JEFF-iron WG

Recently, the JEFF Working Group on iron benchmarking agreed on a list of criticality benchmarks for the validation of iron. This set of benchmarks is given in Table 1 and has been used for testing new ^{56}Fe evaluations. In particular, the *pmi-002.c01* and *hmi-001-1* benchmarks are very sensitive to test the Resolve Resonance (RR) energy region [Cabellos, 2022].

2.3. Selection of criticality Benchmarks for testing the URR

The IAEA/TM on *Code Validation for Generating ACE Libraries* [Trkov 2021] has been working in an intercomparison exercise to test the the processing of nuclear data for neutron transport calculations with Monte Carlo codes in the URR. As a result of this intercomparison exercise, a list of criticality Benchmarks were selected for the validation of the probability tables/multi-band parameters entered by different codes into the ACE libraries (see Table 2). Other Benchmarks have been identified in the recent literature from ICSBEP to assess the impact of the probability tables on important isotopes for fast reactors [García-Herranz, 2021]. Table 3 shows an extract of these Benchmarks excluding those already included in Table 2.

2.4. Selection of LCTs Benchmarks for Criticality Safety Analysis

This section presents the selection of LCT Benchmarks for validation of JEFF-3.3 and ENDF/B-VIII.0 in PWR spent fuel pools and storage casks [JEF/DOC-2041, 2021]. This validation process is conducted in accordance with the recommendations:

- 220 LCTs Benchmarks (see Appendix 3 in [UPM report: 2022-12-20/WP4-D4.6/R6]) as recommended in References: [NUREG/CR-6698, 2001], [Jang, 2018].
- Representative of the typical range of physical parameters (wt%^{235}U, pitch, H/U, EALF, Boron) characterizing PWR spent fuel pools and storage casks with low-enriched UO_2 fuel assemblies.

Table 4 shows the KL (lower tolerance limit) and USL (Upper Safety Limit) predicted with JEFF-3.3 and ENDF/B-VIII.0 using the methodology defined in Ref. [NUREG/CR-6698, 2001]. The difference "K_L(JEFF-3.3) – K_L(ENDF/B-VIII.0)" is only -37 pcm.

Table 1. Iron-Benchmark suite of the WG-JEFF4 on Benchmarking (October 2022)

Case	Benchmark k_{eff}	EALF	Thickness of reflector (mm)	Integral Sensitivity Fe56 capture	Integral Sensitivity Fe56 scattering	Experimental Unc
hmi-001-1	0.9966	31760		-0.1185	0.1726	0.0026
hmf-043-001	0.9995	886000	10		0.0179	0.0018
hmf-043-002	0.9995	878000	20		0.0309	0.0019
hmf-084-007	0.9995	855000	25		0.0642	0.002
hmf-021-001	1	796000	100		0.0986	0.0024
hmf-061-001	0.9998	309000			0.0452	0.0025
hmm-018-002	0.9993	2710		-0.0533	-0.018	0.0007
imf-005-001	1	647000		-0.0007	0.0908	0.0021
mmf-011-001	0.9897	297000		-0.0052	0.0411	0.0023
mmi-003-001	0.9638	29900		-0.0218	0.1202	0.0027
pmf-025-001	1	1270000	15.5	-0.0001	0.0448	0.002
pmf-032-1	1	1250000	45	-0.0002	0.0654	0.002
pmf-026-001	1	1160000	119	-0.0008	0.1214	0.0024
pmf-028-1	1	1120000	200	-0.0015	0.1156	0.0022
pmf-033-001	0.9967	422000		-0.0029	0.0445	0.0026
pmi-002.c01	0.9878	10200		-0.058	0.1147	0.0023

Table 2. List of criticality Benchmarks from ICSBEP considered in the IAEA/TM on Processing.

No.	ICSBEP Label	Short name	Common name	Comment
1	HEU-MET-FAST-001	hmf001	Godiva	
2	HEU-MET-FAST-002	hmf002-002	Topsy-002	
3	HEU-MET-FAST-003	hmf003-001	Topsy-U_2.0in	Uranium reflector
4	HEU-MET-FAST-003	hmf003-002	Topsy-U_3.0in	Uranium reflector
5	HEU-MET-FAST-003	hmf003-003	Topsy-U_4.0in	Uranium reflector
6	HEU-MET-FAST-003	hmf003-010	Topsy-W_4.5in	Tungsten reflector
7	HEU-MET-FAST-003	hmf003-011	Topsy-W_6.5in	Tungsten reflector
8	HEU-MET-FAST-014	hmf014	VNIIEF-CTF-DU	
9	HEU-MET-FAST-032	hmf032-001	COMET-TU1_3.93in	
10	HEU-MET-FAST-032	hmf032-002	COMET-TU1_3.52in	
11	HEU-MET-FAST-032	hmf032-003	COMET-TU1_1.742in	
12	HEU-MET-FAST-032	hmf032-004	COMET-TU1-0.683in	
13	IEU-COMP-FAST-004	icf004	ZPR-3/12	
14	IEU-MET-FAST-007	imf007	Big_Ten(s)	
15	IEU-MET-FAST-007	imf007d	Big_Ten(detailed)	
16	IEU-MET-FAST-010	imf010	ZPR-6/9(U9)	
17	IEU-MET-FAST-012	imf012	ZPR-3/41	
18	IEU-MET-FAST-013	imf013	ZPR-9/1	Reference for tungsten reflector
19	IEU-MET-FAST-014	imf014-002	ZPR-9/2	Tungsten reflector
20	IEU-MET-FAST-022	imf022-001	FR0_3X-S	
21	IEU-MET-FAST-022	imf022-002	FR0_5-S	
22	IEU-MET-FAST-022	imf022-003	FR0_6A-S	
23	IEU-MET-FAST-022	imf022-004	FR0_7-S	
24	IEU-MET-FAST-022	imf022-005	FR0_8-S	
25	IEU-MET-FAST-022	imf022-006	FR0_9-S	
26	IEU-MET-FAST-022	imf022-007	FR0_10-S	
27	MIX-MISC-FAST-001	mif001-001	BFS-35-1	
28	MIX-MISC-FAST-001	mif001-002	BFS-35-2	
29	MIX-MISC-FAST-001	mif001-003	BFS-35-3	
30	MIX-MISC-FAST-001	mif001-009	BFS-31-4	
31	MIX-MISC-FAST-001	mif001-010	BFS-31-5	
32	MIX-MISC-FAST-001	mif001-011	BFS-42	

Table 3. An extract of the list of criticality Benchmarks from ICSBEP considered to study URR.

No.	ICSBEP Label	Common name	Core materials	Reflector materials
1	HEU -COMP-INTER-003	UH3	HEU (93 wt.%) Hydride	Depleted U, Iron, Beryllium
2	HEU-MET-INTER-006	ZEUS	HEU (93 wt.%), Graphite	Copper
3	IEU-MET-FAST-004	Graphite-Reflected IEU Sphere	IEU (36 wt.%)	Graphite
4	MIX-COMP-FAST-001	ZPR-6 Assembly 7	Mixed (Pu,U)- Oxide, Sodium	Depleted U
5	MIX-COMP-FAST-006	ZPPR-2	Mixed (Pu,U)- Oxide, Sodium	Depleted U, Sodium and Steel
6	PU-COMP-INTER-001	HISS/HPG	Pu (5.3 at.% 240Pu), Graphite, Boron	

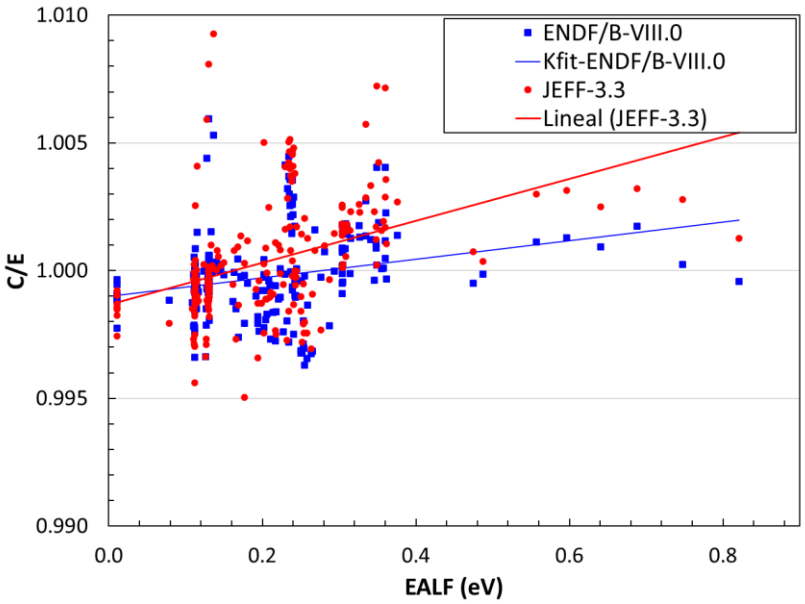

Figure 2. C/E trend as a function of EALF (eV)

Table 4. KL (lower tolerance limit) and USL (Upper Safety Limit) predicted with JEFF-3.3 and ENDF/B-VIII.0

JEFF-3.3		**ENDF/B-VIII.0**	
KL	USL	KL	USL
0.99387	0.94387	0.99424	0.94424

NOTE USL = $K_L - \Delta_{SM}$ (5%) - Δ_{AOA}

2.5. Beyond criticality benchmarks

The use of many integral responses for validation and adjustment with the same type of sensitivities (e.g. k_{eff}) may provoke some uncovered compensating errors between various nuclear-data observables. Therefore, different integral observables will give us different sensitivities to the same nuclear data compared to those of a unique response (e.g. k_{eff}). This will allow us to avoid potential compensation errors in the adjustment/tuning of nuclear data [JEF/DOC-2015, 2020], [IAEA/INDEN-Nov 2020].

So, one can combine different integral benchmarks to partially disentangle the bias in a set of experiments. For instance, the sensitivity of k_{eff} to $\bar{\nu}$ or (n,fission) is very similar in criticality benchmarks. The same can be said for prompt fission neutron spectrum and (n,n'). To disentangle this effect, it is needed other type of integral benchmark experiment with different sensitivities to these nuclear data in the same energy range.

- Criticality and **reaction rates/spectral indexes**

Table 5 shows results for the Big-10 benchmark. This case is used to show the differences in ^{238}U/URR evaluation between JEFF-3.3 and ENDF/B-VIII.0. Here, reaction rates (RRs) and criticality values are compared with measurements. C/E values for k_{eff} show a good agreement both in JEFF-3.3 and ENDF/B-VIII.0 However, JEFF-3.3 gives an underestimation of 8% and 10% in the reaction rates of C28/F25 and F28/F25, respectively. It can be attributed to the different compensation in criticality and RRs for each cross-section channel in these experimental values.

A second example is shown in Table 6 for the Jezebel Benchmark with ^{239}Pu nuclear data. As it can be seen in Table 5 and Table 6, nuclear data both in JEFF-3.3 and ENDF/B-VIII.0 predicted quite well k_{eff}. So, it gives some indications that nuclear data were tweaked by evaluators.

Both JEFF-3.3 and ENDF/B-VIII.0 may have some compensations in the nuclear data to predict the same (approximately) k_{eff} value. However, the underestimation of C28/F25 may give us some indications that a better evaluation can be still performed. Figure 3 shows the sensitivity profiles for k_{eff} and C28/F25 reaction rates for the same cross-section ^{235}U(n,fission) in Godiva (HMF1) Benchmark. It gives a different trend for different response. The Figure also shows the C28/F25 sensitivity for ^{235}U(n,fission) in Jezebel (PMF1) Benchmark showing similar trend in different Benchmarks.

- **The necessity of an extended set of criticality benchmarks to give some indications on specific isotopes-reactions**

There is a necessity of extended ICSBEP validation suites to identify trends in nuclear data evaluations [JEFF-CG, April 2020]. This is the case of PST-034 benchmarks (Figure 4) which are used to show the impact of different evaluations for the 239Pu in the energy range between 0.1eV and 1eV. The sensitivity to the 239Pu cross-sections is very large due to the large amount of 239Pu, the thermal energy range is also controlled with different amounts of Gd in the Benchmark.

As it can be observed in Figure 4, JEFF-3.3 shows an overestimation in keff between 500-750 pcm for the cases PST-0034-007 to 015. However, ENDFB/B-VIII.0 shows an underestimation in keff between 250-500 pcm. These large deviation in JEFF-3.3 respect to ENDF/B-VIII.0 is justified because of the differences around the first resonance in the JEFF-3.3 evaluation.

Table 5. Criticality and reactions rates in IEU-MET-FAST-007: Big-10.

Quantity	$\Delta E_{exp}/E$	C/E	
		JEFF-3.3	ENDF/B-VIII.0
$^{238}U(n,f) / ^{235}U(n,f)$ = F28/F25	± 0.02	0.90	0.96
$^{238}U(n,g) / ^{235}U(n,f)$ = C28/F25	± 0.03	0.92	0.96
k_{eff} (detailed model)	± 70 (pcm)	1.00041	0.99979
k_{eff} (Improved simplified model)	± 80 (pcm)	0.99997	0.99951

Table 6. Criticality and reactions rates in PU-MET-FAST-001

Quantity	$\Delta E_{exp}/E$	C/E	
		JEFF-3.3	ENDF/B-VIII.0
$^{238}U(n,f) / ^{235}U(n,f)$ = F28/F25	± 0.01	0.98	0.99
$^{238}U(n,g) / ^{235}U(n,f)$ = C28/F25	---	0.93	0.95
$^{237}Np(n,f) / ^{235}U(n,f)$ = F37/F25	± 0.01	1.00	0.99
$^{239}Pu(n,f) / ^{235}U(n,f)$ = P49/F25	± 0.01	0.98	0.98
k_{eff} (simple model. rev4)	± 110 (pcm)	1.00020 ± 0.00002	1.00067 ± 0.00002

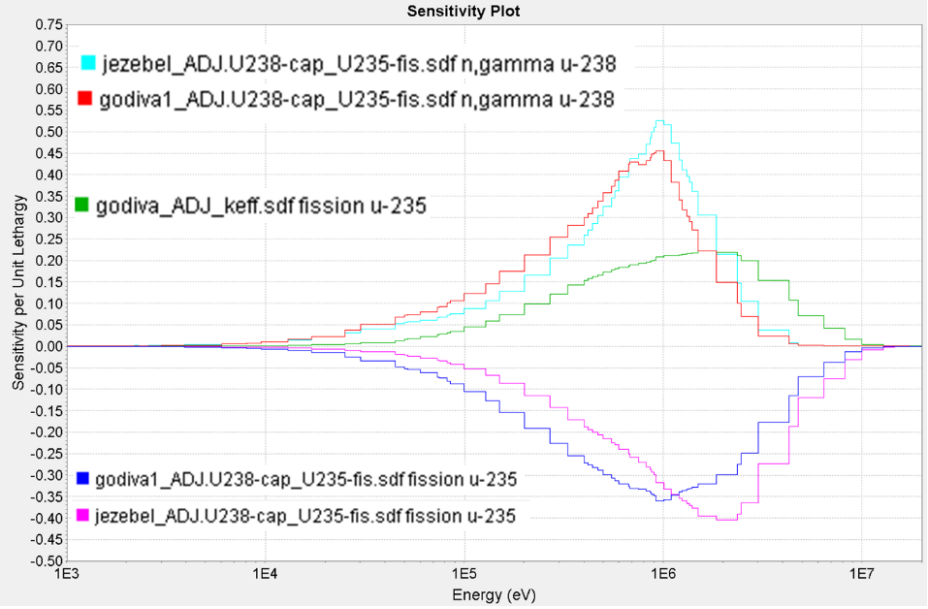

Figure 3. Sensitivity profiles for C28/F25 in Jezebel and Godiva and k_{eff} in Godiva

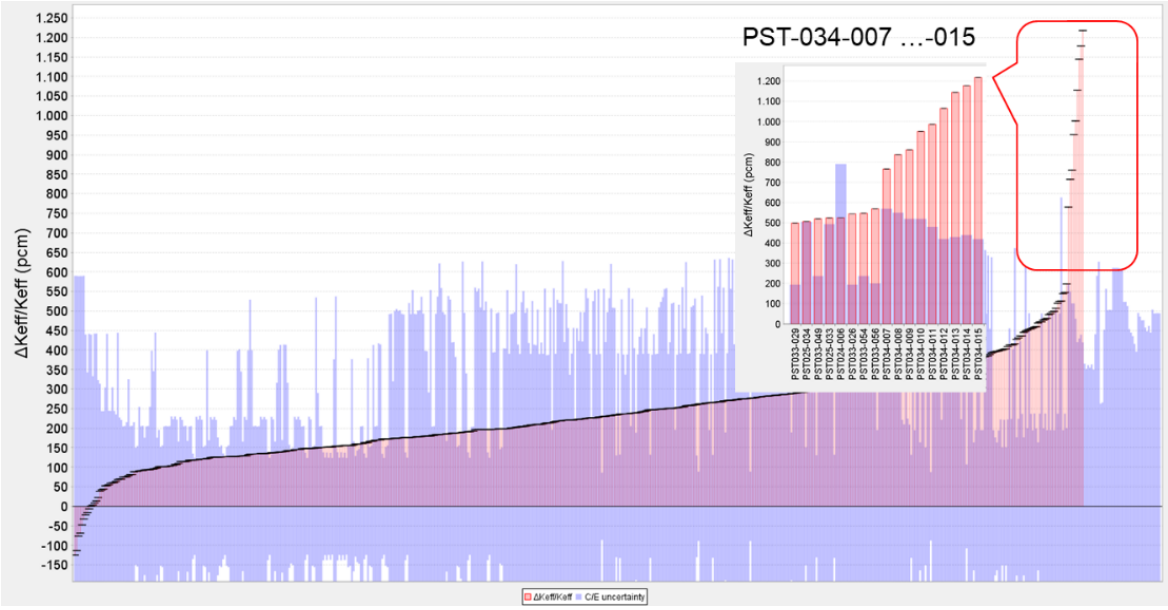

Figure 4. $\Delta k_{eff}/k_{eff}$ in pcm due to changes "only" in ^{239}Pu between JEFF-3.3 and ENDF/B-VIII.0 as a function of the full set of PU Benchmarks in ICSBEP.

- **Depletion benchmarks: PIE and reactivity.**

The use of depletion benchmarks can give some insights to different nuclear data trends where the sensitivities might differ from criticality cases. Here, post-irradiation-experiments (PIE) can be used for nuclear data validation (e.g. SFCOMPO database, which will be described in more detail in section 5). Unfortunately, reactivity values (k_{eff}) of those depleted benchmarks are not available in the current databases and hence computational benchmarks have to be used to give additional indications on nuclear data.

In depletion calculations, the problem is a time dependent problem where sensitivities and correlations change over time. Hence, we need sensitivities to assess the impact of changes both in the reactivity and in the isotopic inventory (e.g. ^{239}Pu) due to different nuclear data evaluations

Similarity indexes (e.g. ck-values) can be used to find criticality benchmarks with a similar trend to depletion. That is the case of PST-034 cases which shows a similarity of ck~0.95 with the reactivity change in depletion at high burnups for the ^{239}Pu thermal cross-sections.

- **Neutron transmission experiments**

Other indications on nuclear data can be found using neutron transmission experiments. For instance, there are benchmarks at ICSBEP/FUND-JINR-1/E-MULT-TRANS-001 which can be used. This type of experiments can show some trends in the α-value ($\alpha = \sigma_\gamma / \sigma_f$) characterized by different self-shielded and unshielded experiments. Therefore, transmission benchmarks can give us some additional insight to different nuclear data because their sensitivities differ from criticality.

- **Shielding Benchmarks**

Examples such as LLNL pulsed spheres, OKTAVIAN/ToF and FNS/ToF experiments may give us additional insights above 2 MeV, i.e. above the neutron energy of criticality benchmarks. These shielding benchmarks are focused on specific nuclear data such as scattering (elastic, inelastic) and fission observables (fission cross sections, $\bar{\nu}$ and prompt fission neutron spectrum). But once again, one cannot disentangle deficiencies in these nuclear data using only pulsed spheres. Additional experiments, including differential ones are needed. A detailed overview of the SINBAD database of shielding benchmark experiments in given in Section 3.

One difficulty with these shielding and transmission benchmarks is that they have a high sensitivity to neutron leakage which may create further shortcomings if deficiencies in angular distributions are compensated in the integral-energy cross-sections. Consequently, the sensitivity to angular distributions is crucial to disentangle the contributions in the correct prediction of neutron leakages due to angular and integral nuclear reaction data.

- **Kinetic Benchmarks**

Finally, another family of integral experimental data that can also be used for nuclear data validation are kinetic parameters, namely the effective delayed neutron fraction and mean neutron generation time. The reference database for finding this information should be, in principle, OECD/NEA maintained International Handbook of Evaluated Reactor Physics Benchmark Experiments (IRPhE), but actually very few experimental kinetic information is contained in it. The use of these experiments for benchmarking is discussed in section 4. Some specific features of kinetic benchmarks making their use in ND improvement studies complementary to other experiments are presented in [Kodeli, 2017], [Kodeli, 2018].

2.6. References

[Cabellos, 2022] O. Cabellos, *Sensitivity Analysis for ^{56}Fe(n,gamma) in criticality Benchmarks*, JEFF Meeting on iron evaluation, November 9, 2022

[García-Herranz, 2021] N. García-Herranz *et al.*, *Diagnosis of the Unresolved Domain treatment in Monte Carlo Transport Calculations trough the Identification and Modelling of Criticality Safety Experiments*. In Proceedings of PHYSOR2020, EPJ Web of Conferences 247 (2021) 10003.

[ICSBEP, 2009] J. Briggs (ed.), *International Handbook of Evaluated Criticality Safety Benchmark Experiments*. Organization for Economic Cooperation and Development—Nuclear Energy Agency (OECDNEA) (2009)

[IAEA/INDEN-Nov 2020] O. Cabellos, *Indications from integral benchmarks on U-235, U-238 and Pu-239 evaluations*, IAEA CM of the INDEN on Actinide Evaluation in the Resonance Region, 17-19 Nov 2020 (video-conference)

[Jang, 2018] Jaerim Jang *et al.*, *Validation of UNIST Monte Carlo code MCS for criticality safety analysis of PWR spent fuel pool and storage cask*. Annals of Nuclear Energy 114 (2018) 495-509.

[JEFF-3.3, 2018] A. Plompen *et al.*, *The joint evaluated fission and fusion nuclear data library, JEFF-3.3*, Eur. Phys. J. A 56 (2020) 181.

[JEF/DOC-2015, 2020] O. Cabellos, M. García-Hormigos, B. Moreno and S. Sánchez-Fernández, *The importance of using different integral benchmarks to provide valuable feedbacks to the evaluation process*. JEFF Meeting and JEFF-CG, Nov 2020. JEFDOC-2015 (video-conference).

[JEF/DOC-2041, 2021] O. Cabellos, *Overview of Processing, Verification and Benchmarking activities at UPM*. JEFF Meeting, April 28, 2021. JEFDOC-2041 (video-conference).

[JEFF-CG, April 2020] O. Cabellos, *PU-ICSBEP Benchmarking in Thermal Energy Spectrum… Identifying ICSBEP Benchmarks to point out the issue of 239Pu in JEFF-3.3*. JEFF-CG, JEFF Meetings, April 28, 2020 (video- conference)

[JEFF-Validation, 2022] https://git.oecd-nea.org/databank/nds/jeff/jeff-validation/benchmarks

[Kodeli, 2017] I. Kodeli, *Combined use of k-effective and beta-effective measurements for nuclear data validation and improvement*. In Proceedings of Int. Conf. On Nuclear Data for Science and Technology (ND2016) 11-16 Sept. 2016, Bruges (Belgium). EPJ Web of Conferences 146 (2017) 06018.

[Kodeli, 2018] I. Kodeli and L. Plevnik, *Nuclear data adjustment exercise combining information from shielding, critical and kinetics benchmark experiments ASPIS-Iron 88, Popsy and SNEAK-7A/7B*, Progress in Nuclear Energy 106 (2018) 215 – 230.

[LA-UR-11-05076] R.D. Mosteller, F.B. Brown and B.C. Kiedrowski, *An expanded criticality validation suite for MCNP*. Los Alamos National Laboratory LA-UR-11-05076 (2011).

[Mosteller, 2005] R.D. Mosteller, *Comparison of results from the MCNP criticality validation suite using ENDF/B-VI and preliminary ENDF/BVII nuclear data*. In Proceedings of Int. Conf. On Nuclear Data for Science and Technology (ND2004), Sep. 26 – Oct. 1, 2004, Santa Fe (USA).

[NUREG/CR-6698, 2001] J.C. Dean and R.W. Tayloe Jr., *Guide for Validation of Nuclear Criticality Safety Calculational Methodology*. NUREG CR-6698. U.S. Nuclear Regulatory Commission, 2001 NUREG/CR-6698

[Romojaro, 2022] P. Romojaro *et al.*, *Report on ESFR, MYRRHA, and ALFRED sensitivity and impact studies*. EU H2020 SANDA project deliverable D5.2, issued on 25/10/2022.

[Trkov, 2021] A. Trkov, *Current Achievements of the Code Verification Project for Generating ACE Libraries*, Technical Meeting on Nuclear Data Processing, 18-22 October 2021, IAEA Headquarters, Vienna (Austria).

[UPM report: 2022-12-20/WP4-D4.6/R6] O. Cabellos, *Review of Benchmarks for nuclear data validation*, UPM report: 2022-12-20/WP4-D4.6/R6.

3. SINBAD shielding benchmarks

The "lifetime" of well-defined benchmark experiments is usually much longer than that of nuclear data libraries, basic data evaluations and computer codes and methods. Although designed to validate some specific computational methods and data at a given time, benchmark experiments do not become obsolete but can very well serve for testing further methods or data that will be developed and produced later. This shows the importance of preserving and making easily accessible the information on these benchmarks.

Creation of a shielding benchmark database was first announced in 1988 at the Seventh International Conference on Radiation Shielding (ICRS7) in Bournemouth, UK [Miller,1988], following the discussions within a series of specialists' meetings organised in 1980s by NEACRP in Paris and Saclay. The SINBAD project (A Shielding Integral Benchmark Archive and Database) [Kodeli, 2021], [sinbad] was then started in the early 1990's as a joint project of the OECD/NEA Data Bank and Oak Ridge National Laboratory's Radiation Safety Information Computational Center (RSICC) with the objective to develop an electronic data base for storing and retrieving information about the shielding experiments for nuclear systems. The SINBAD database includes description of experiments, experimental results, and calculational models, as well as stores relevant figures and reports in the digitized page image form.

In the first ~15 years a total of about 100 benchmark evaluations were prepared for SINBAD, with 84 evaluations performed by the NEA Data Bank and 18 evaluations by the RSICC. The documentation was independently checked by 2 scientists, however due to limited funding the evaluated benchmark data were of different quality, and with varying degree of rigorousness and completeness of reported experimental information. To provide a better guidance to the users of the database, a detailed quality evaluation of the evaluations was started in 2008 and it is by now completed for about half of the database. Where performed, the main conclusions, including the overall quality note and the identification of missing information such as geometry description, experimental uncertainties etc., are reported.

Computational analyses of the experiments were performed using different radiation transport software – both deterministic and Monte Carlo. Because the experiments were analysed over several years, some of the computer codes are no longer available in the public domain. In some cases, Monte Carlo calculations were compared with deterministic ones. For Monte Carlo, input data for different versions of MCNP-4, 5, 6 are predominant, but others, such as TRIPOLI, SERPENT, MCBEND, GEANT are also available or under preparation. For the deterministic computations, older versions like DOT3.5, DORT-TORT, DANTSYS, PARTISN etc. were typically included. For higher energies, FLUKA, MARS, HETC, LAHET and PHITS were implemented.

A few of the experiments have not been analysed computationally. Annex 2 presents the listing of the experiments in respective categories – Table 23, Table 24 and Table 25 for fission; Table 26 and Table 27 for fusion, and Table 28 and Table 29 for accelerators. In addition, the software used in analysing each experiment is listed in the last column. If the input files for the software are available, it is noted in the last column. In a few cases, the input files are not in digital format, but are listed in the accompanying cited documents.

The OECD NEA Working Party on Scientific Issues of Reactor Systems (WPRS) Expert Group on Radiation Transport and Shielding was started around 2011 with the mandate, among others, to monitor, steer and support the continued development of the SINBAD database.

Since its inception in the 1990's, SINBAD has grown by ~2009 into a collection of 102 benchmarks, comprising 48 fission, 31 fusion and 23 accelerator experiments. Many scientists from varied countries contribute to the SINBAD collection. After ~2009 the database was managed in the scope of EGPRS, however little new data was added, focussing the discussion on improving and modifying the general format of the data. Lack of maintenance resulted in a reduced use of shielding benchmarks in nuclear data V&V procedure, which was mainly based on easily available and ready-to-use ICSBEP/IRPhE [IRPhE, 2019] critical benchmarks. To improve this situation and promote a wider use of SINBAD, the OECD/NEA WPEC Sub-group 47 [WPEC47a, 2019], [WPEC47b, 2022] was started in 2019, followed in January 2022 by a SINBAD Task Force to carry on the work on further development of SINBAD hopefully incorporating some recommendations from WPEC SG47.

3.1. Organisation of the SINBAD database

Several new evaluations are at present ongoing as part of the SINBAD Task Force: FNG Copper, FNG HCLL, KFK gamma Fe sphere, Oxygen Broomstick, TIARA etc. These evaluations are going through a thorough review and will be released on GitHub platform when/if successfully passing. The formats used in the old and the new sets of SINBAD evaluations also differ.

The presently available SINBAD benchmark data are distributed by NEADB as part of the following packages:

- NEA-1517 SINBAD REACTOR
- NEA-1552 SINBAD ACCELERATOR
- NEA-1553 SINBAD FUSION

Each experiment in the "old" SINBAD collection has the following descriptive properties:

a) Contributor
b) Name of experiment
c) Purpose of the experiment
d) Description of the source and experimental configuration
e) Measurement system and uncertainties
f) Results and Analysis; comparison with calculations

3.1.1. Old format as used in the 102 available SINBAD benchmark evaluations:

The presently available (102) evaluations in SINBAD are structured around the following main files:

- INDEX
- ABSTRACT
- BENCHMARK EVALUATION file
- Supplementary supporting documentation (original reports, drawings, computer code inputs, quality evaluation reports)

I. SINBAD INDEX

SINBAD INDEX file contains the list of all available benchmark experiments in SINBAD which can be sorted by alphabetical name, shielding application (fission/fusion /accelerators), shielding material, laboratory and the year when the experiment was completed. Acknowledgement is given to the contributing laboratories. The file includes HTML format hyperlinks pointing to Abstract files of individual benchmarks.

II. SINBAD ABSTRACT

SINBAD ABSTRACT provides the general descriptors of the experiments, a list of all the data and documents available in the evaluation with hyperlinks. It is organized around ten main sections listed in Table 7.

III. BENCHMARK EVALUATION REPORT

SINBAD EVALUATION REPORT is the main document including the description and evaluation of the benchmark information. The evaluation reports are in HTML format and can include hyperlinks to drawings and data files that are presented or summarized in other files. The presently available (102) evaluation documents are prepared in free format without very strict structure and chapter definitions. The main (HTML) documents generally includes, as a minimum, chapters on:

- Radiation source
- Shield and its environment
- Detector system
- Measurement results with uncertainties

As mentioned above, some (51) SINBAD evaluations include in addition a quality evaluation report with a thorough review and detailed information on:

- Radiation source
- Shield and environment
- Instrumentation (detector geometry, experimental methods, measurement uncertainties.
- Benchmark data and computational models.

Quality reports are included as separate PDF documents, although it was planned to integrate them in the benchmark evaluation report at the later stage.

Benchmark model specifications are in most present evaluations not complete since it was expected that the computational models would evolve and become more sophisticated with the improvement of computational capabilities. For the older benchmarks the simplified versions are described which were used at the time when the experiments were performed, and do not take into account the new modelling possibilities. The modelling capabilities of modern computer codes and their possible contribution to improve the modelling of the benchmark were investigated during the quality evaluation of the experiments and are discussed in the Quality evaluation reports where available.

3.1.2. New SINBAD formats

Modifications of the above SINBAD format or adopting a new format was discussed since 2012 within the EGPRS. Two new formats were proposed (shown on Table 8 and Table 9) which still included the SINBAD INDEX and ABSTRACT files that provide an overview of the database, general descriptors of the experiments and hyperlinks to the available evaluation reports, computer code inputs and other background data. Finally, at the ICSBEP/IRPhE meeting in 2019 another format largely inspired by (practically the same as) the one used for criticality benchmark evaluations of IRPhE (International Reactor Physics Experiment Evaluation Project) and ICSBEP (International Criticality Safety Benchmark Evaluation Project) was adopted for future evaluations. The format is given in Table 10. The new format is however not compatible with the old one, since the files INDEX and ABSTRACT are not used any more. Further inconvenience for the users is that some shielding benchmarks are also evaluated in the IRPhE database. In the past some evaluations were shared between SINBAD and IRPhE. For example, the VENUS-3 and Baikal-1 Skyshine Benchmarks were first released within SINBAD project and a more thorough evaluation was later performed in the scope of the ICSBEP project. These two evaluations are now shared with ICSBEP, provided in a slightly different format (basically with only ABSTRACT file added in SINBAD), with a clear updating policy and responsibilities. However, such sharing of evaluations among databases is not planned for future.

Users are therefore advised to consult all three databases for shielding benchmarks suitable for a particular application.

3.2. Quality evaluations

Since the experimental data presently available in SINBAD are of varying quality, a thorough revision and classification of the benchmark experiments was undertaken under the guidance of the NEA Data Bank in order to provide users with easier choices and help them make better use of the experimental information. The main criteria used in the review are the completeness and consistency of information, in particular concerning the evaluation of the experimental sources of uncertainty. These concern the experimental setup, the neutron source specifications, the detector characteristics, the geometry and precise material composition of the components. Between 2008 and 2014 the review was concluded for 52 benchmark experiments, mostly of relevance for fusion neutronics (25), but also for fission (17) and for accelerator shields (10). The outcomes of this work are described in [Milocco, 2010], [Milocco, 2010a], [Milocco, 2013], [Milocco, 2015], [Zerovnik, 2015]. The concerned experiments are given in Annex 3. 45 experiments were revised and updated SINBAD

compilations released (2008-2011). Six fission reactor and accelerator benchmarks were revised, but the revisions are not yet included in SINBAD. The review was focused on:

- New experimental information from the literature.
- Refinement of source model where possible.
- New MCNP models reproducing the experiment as exactly as reasonably possible, avoiding unnecessary approximations.
- Sensitivity studies to study the impact of neutron source description, composition and geometry uncertainties where available.

3.3. Examples of benchmark analyses

Although less widely used compared to the ICSBEP and IRPhE benchmarks, SINBAD benchmarks still proved useful for computer code and nuclear data validation and improvement. Interest in SINBAD integral benchmark data was expressed in the scope of projects of the European Commission CHANDA, F4E, OECD WPEC, FENDL etc. Recent examples of SINBAD benchmarks include the validation of different nuclear data validation, such as JEFF-3.3 [4], -4T, CIELO, ENDF/BVIII.0, FENDL-3.2 [6], IRDFF-II [7] and JENDL-4.0, -5. Some V&V analyses are reported in [jefdoc-2175, 2022], [jefdoc-2141, 2022], [effdoc-1462, 2021], [jefdoc-2044, 2021], [jefdoc-2016,2020], [jefdoc-1854, 2017], [jefdoc-1807, 2017], [Kodeli, 2023], [Kodeli, 2019], [Kodeli, 2018], [Schnabel, 2023] using the following shielding benchmarks:

- ASPIS Fe88,
- PCA Replica
- PCA ORNL
- CIAE neutron leakage spectra from Fe
- KFK 1977 gamma fields in iron spheres
- FNG-HCLL Tritium Breeder Module Mock-up
- FNG-Copper
- FNG-WCLL

Table 7. SINBAD ABSTRACT content.

Section	Title
1	Name of the Experiment
2	Purpose and Phenomena Tested
3	Description of the Source and Experimental Configuration
4	Measurement System and Uncertainties
5	Description and Results of Analysis
5a	Benchmark model
6	Quality assessment (review)
6a	Special Features
7	Author/Organizer
8	Availability
9	References
10	Data and Format

Table 8. Option one for the format of the evaluation report discussed within EGPRS in 2011-2017.

Section	Title
1.	DETAILED DESCRIPTION
1.1	Description of the Experiment
1.1.1	Overview of the Experiment
1.1.2	Facility Description
1.1.3	Measurement Methods
1.1.4	Summary of Evaluation and Recommendation
1.2	Attributes of the Experiment
1.2.1	Description of the Measurement Methods and Data Reduction Process
1.2.2	Description of Measurement Uncertainties
1.3	Description of Experimental Configuration
1.3.1	Description of the Source
1.3.2	Description of the Shield and Facility
1.3.3	Description of the Detection System
1.4	Measurement Information
1.4.1	Measured Parameters and Uncertainty
1.4.2	Measurement Processing Procedures and Results
1.4.3	Calibration, Efficiency and Detector Property Analysis
1.4.4	Additional Measurement Information
1.5	Interpretation of Measurements
1.5.1	Derived Measurements
1.5.2	Uncertainties in Derived Measurements
1.5.3	Additional Information
2.	(Quality) EVALUATION OF EXPERIMENTAL DATA
2.1	Evaluation of Experimental Configuration
2.1.1	Evaluation of Source Description
2.1.2	Evaluation of Shield Configuration
2.1.3	Evaluation of Detector System
2.1.4	Evaluation of Facility Effects
2.2	Evaluation of the Measured Data
2.3	Sensitivity and Uncertainty Analysis
2.3.1	Calculated Model
2.3.2	Sensitivity Analysis
2.3.3	Overall Uncertainty
2.4	Evaluation Conclusions and Recommendations
3.	BENCHMARK SPECIFICATIONS
3.1	Benchmark Model Specifications for Shielding Measurements
3.1.1	Description of Benchmark Model Simplifications
3.2	Source Description
3.3	Shield Description
3.4	Shield Material Data
3.5	Detection System
3.6	Facility Description
4.0	RESULTS OF SAMPLE CALCULATIONS (& NUCLEAR DATA SENSITIVITIES) (Optional)
6.0	REFERENCES
	APPENDICES (Optional)

Table 9. Option two for the format of the evaluation report.

Section	Title
1.	SINBAD Experiment Description File
1.1	Description of the Source
1.2	Description of the Shield and Facility
1.3	Description of the Detection System
1.4	Experimental Results
1.4.1	Measured Parameters and Uncertainty
1.4.2	Measurement Processing Procedures and Results
1.4.3	Calibration, Efficiency and Detector Property Analysis
1.4.4	Additional Measurement Information
1.5	Interpretation of Measurements
1.5.1	Derived Measurements
1.5.2	Uncertainties in Derived Measurements
1.5.3	Additional Information
2.	QUALITY EVALUATION
2.1	Evaluation of Experimental Configuration
2.1.1	Evaluation of Source Description
2.1.2	Evaluation of Shield Configuration
2.1.3	Evaluation of Detector System
2.1.4	Evaluation of Facility Effects
2.2	Evaluation of the Measured Data
2.3	Sensitivity and Uncertainty Analysis
2.3.1	Calculated Model
2.3.2	Sensitivity Analysis
2.3.3	Overall Uncertainty
2.4	Evaluation Conclusions and Recommendations
3.	BENCHMARK (MODEL) SPECIFICATIONS
3.1	Benchmark Model Specifications for Shielding Measurements
3.1.1	Description of Benchmark Model Simplifications
3.2	Source Description
3.3	Shield Description
3.4	Shield Material Data
3.5	Detection System
3.6	Facility Description
4.	CALCULATIONS (& NUCLEAR DATA SENSITIVITIES) (Optional)

Table 10. New ICSBEP/SINBAD format adopted at ICSBEP/IRPhE/SINBAD TPR meeting, inspired by the IRPhE Project format.

Section	Title
1	EXPERIMENT DESCRIPTION
1.1	Description of the experiment
1.1.1	Overview of the experiment (Place, Institution, Persons & tasks)
1.1.2	Facility description (Room, dimensions, source position)
1.1.3	Measurement methods
1.1.4	Measurement evaluation identification
1.2	Description of each measurement configuration
1.2.1	The source
1.2.2	The shield
1.2.3	The detection system
1.3	Description of materials and radiation sources
1.3.1	Description of the source
1.3.2	Description of the shield
1.3.3	Materials of the detection system
1.4	Measurement of input and output variables
1.4.1	Neutron source intensity
1.4.2	Activation of foils irradiated by neutrons
1.4.3	Total dose measured with TLD
1.4.4	Neutron flux measured with proportional counters
1.4.5	Neutron spectrum measured with Bonner spheres
1.4.6	Neutron spectrum measured by time-of-flight
1.4.7	Neutron spectrum measured with plastic scintillator
1.4.8	Tritium production measured by liquid scintillator
1.4.9	Tritium production measured by difference in TLD dose
1.4.10	Tritium production measured by self-irradiated TLD
1.5	Additional information
2	EVALUATION OF MEASURED DATA
2.1	Evaluation of the measurement configuration
2.1.1	Configuration geometry parameter values
2.1.2	Material characteristics parameter values
2.1.3	Radiation source parameter values
2.1.4	Evaluation of uncertainties of the experimental configuration parameters
2.2	Evaluation of the measured data
2.2.1	Activation of foils
2.2.2	Total dose measured by TLD
2.2.3	Neutron flux measured with proportional counter
2.2.4	Neutron spectrum measured with Bonner spheres
2.2.5	Neutron spectrum measured by time-of-flight
2.2.6	Neutron spectrum measured with plastic scintillator
2.2.7	Tritium production measured by liquid scintillator
2.2.8	Tritium production measured by difference in TLD dose
2.2.9	Tritium production measured by self-irradiated TLD
2.3	Sensitivity and uncertainty analysis
2.3.1	Calculation model

2.3.2	Sensitivity to the source characteristics
2.3.3	Sensitivity to the physical parameters of the shield
2.3.4	Summary of sensitivity analysis
2.3.5	Total uncertainty
3	BENCHMARK MODEL
3.1	Description of the different benchmark models
3.2	Source and target description
3.3	Shield description
3.4	Shield material data
3.5	Detection system
3.6	Materials of the detection system
3.7	Facility description
3.8	Benchmark model values for total dose with TLD
3.9	Benchmark model values for neutron flux with proportional counter
3.10	Benchmark model values for neutron spectrum with Bonner spheres
3.11	Benchmark model values for neutron spectrum with time-of-flight
3.12	Benchmark model values for neutron spectrum with plastic scintillator
3.13	Benchmark model values for tritium production with liquid scintillator
3.14	Benchmark model values for tritium production by difference in TLD dose
3.15	Benchmark model values for tritium production by TLD self-irradiation
4	SAMPLE CALCULATIONS
4.1	Results for benchmark model A with code A
4.2	Results for benchmark model B with code B
4.3	Results for benchmark model A with code A
4.4	...

3.4. References

[IRPhE, 2019] J.D. Bess, T. Ivanova, J. Hill, L. Scott, The 2019 Edition of the IRPhEP Handbook. United States: N. p., 2019. Web.

[jefdoc-2175, 2022] I. Kodeli, Validation of Fe nuclear data using SINBAD benchmarks and neutron and gamma ND sensitivity - uncertainty analysis, JEFDOC-2175, Issy-les-Moulineaux, 21 Nov. 2022

[jefdoc-2141, 2022] I. Kodeli, V&V of JEFF-4T and FENDL-3.2a iron cross sections against shielding benchmarks, JEFDOC-2141, 27 April 2022

[effdoc-1462, 2021] I. Kodeli, FNG-WCLL benchmark: possible reasons for ^{197}Au vs. ^{186}W(n,γ) C/E discrepancies from a S/U point of view, EFFDOC-1462, NEA, 24 Nov. 2021

[jefdoc-2044, 2021] I. Kodeli, Validation of iron cross sections using PCA replica shielding benchmarks, JEFDOC-2044, NEA, April 2021

[jefdoc-2016,2020] S.C. van der Marck, Results for the PCA Pressure Vessel Facility Benchmark, JEFDOC-2016, NEA, Nov. 2020

[jefdoc-1854, 2017] I. Kodeli, Iron Nuclear Data Testing Using SINBAD Shielding Experiments, JEF/DOC-1854, NEA, April 2017

[jefdoc-1807, 2017] I. Kodeli, ASPIS-Iron88 benchmark results using different cross-section evaluations including JEFF-3.3T2, JEF/DOC-1807, Nov. 2016

[Kodeli, 2023] I.A. Kodeli, S. van der Marck, Consistency among the results of the ASPIS Iron88, PCA Replica and PCA ORNL benchmark results, Nucl. Sci. Eng. (accepted, to appear)

[Kodeli, 2021] I. A. Kodeli, E. Sartori, SINBAD - Radiation shielding benchmark experiments, Annals of Nuclear Energy 159 (2021) 108254

[Kodeli, 2019] I. Kodeli, M. Angelone, FNG Copper Benchmark Evaluation for the SINBAD Database, *Fusion Engineering and Design* 146 (2019) 312-315

[Kodeli, 2018] I. Kodeli, Transport and S/U analysis of the ASPIS-IRON88 Benchmark using recent and older iron cross-section evaluations. V: PHYSOR 2018, PHYSOR 2018, Reactor physics paving the way towards more efficient systems, 22 - 26 April 2018, Cancun, Mexico.

[Kodeli, 2018a] I. Kodeli, Introduction to SINBAD – tutorial, Proc. *RPSD-2018: 20th Topical meeting of the radiation protection and shielding division*. American Nuclear Society, Inc. 2018.

[Kodeli, 2016] I. Kodeli, K. Kondo, R.L. Perel, U. Fischer, Cross-Section Sensitivity and Uncertainty Analysis of the FNG Copper Benchmark Experiment, *Fusion Engineering and Design*, 109-111 (2016) 1222-1226.

[Miller, 1988] P. Miller, P. Nagel, M. Salvatores, E. Sartori: Shielding Experimental Benchmark Base at the Nuclear Energy Data Bank, Proc: 7th Int. Conf. on Rad. Shielding, Bournemouth, UK 1988 NEACRP-L-310

[Milocco, 2010] A. Milocco, A. Trkov, I. Kodeli, The OKTAVIAN TOF experiments in SINBAD: Evaluation of the experimental uncertainties, *Annals of Nuclear Energy* 37 (2010) 443-449

[Milocco, 2010a] A. Milocco, I. Kodeli, A. Trkov, The 2010 Compilation of SINBAD: Quality Assessment of the Fusion Shielding Benchmarks, Proc. NEMEA-6 Scientific workshop on Nuclear Measurements, Evaluations and Application, Krakow, Poland, 25-28 October 2010.

[Milocco, 2013] A. Milocco, A. Trkov, I. Kodeli, Quality Assessment of Evaluated Experiments Nesdip-2, Nesdip-3, Janus-1, Janus-8, Proc. 22nd Int. Conf. Nuclear Energy for New Europe, Bled, Sept. 9-12, 2013

[Milocco, 2015] A. Milocco, Quality Assessment of SINBAD Evaluated Experiments ASPIS Iron, ASPIS Iron-88, ASPIS Graphite, ASPIS Water, ASPIS N/G Water/Steel, ASPIS PCA Replica, Dec. 2015.

[Schnabel, 2023] G. Schnabel, et al., FENDL: A library for fusion research and applications, Nucl. Data Sheets (to be published)

[sinbad] SINBAD database, OECD-NEA, available online: *https://oecd-nea.org/science/wprs/shielding/sinbad/sinbadis.htm*

[WPEC47a, 2019] I. Kodeli, O. Cabellos, L. Leal, Use of Shielding Integral Benchmark Archive and Database for Nuclear Data Validation, Web of Conferences, 14th International conference on nuclear data for science and technology (ND2019), 19 May, 2019, Beijing.

[WPEC47b, 2022] I. Kodeli, M. Fleming, O. Cabellos, L. Leal, Y. Celik, Y. Ding, B. Jansky, D. Neudecker, E. Novak, S. Simakov, Y. Iwamoto, A. Valentine, Outcomes of WPEC SG47 on "Use of Shielding Integral Benchmark Archive and Database for Nuclear Data Validation", Proc. Int. Conf. on nuclear data for science and technology (ND2022), July 25-29, 2022.

[Zerovnik, 2015] G. Žerovnik, I. Kodeli, A. Trkov, A. Jazbec, Re-evaluation of the EURACOS integral shielding experiment series, *Annals of Nuclear Energy*, 77, 318-325, 2015.

4. Kinetic parameter benchmarks

As stated above, kinetic parameters (namely, the effective delayed neutron fraction β_{eff} and mean neutron generation time Λ_{eff}) can also be used for validation of nuclear data and complement traditional nuclear data validation using k_{eff}, as described in section 2. For the purposes of SANDA T4.4, a search of such benchmarks has been carried out and a sensitivity and uncertainty (S/U) analysis has been performed in order to determine level of nuclear data sensitivity. In addition to this, a good knowledge of reactor kinetic parameters and their uncertainty is also relevant in other fields, such as nuclear reactor safety or reactivity monitoring of accelerator-driven systems (ADS). The results of this work are fully presented in [Bécares 2022]; here the main findings are summarized.

4.1. Methodology

Although experimental kinetic information is in principle included in the IRPhE [NEA 2020b] database, actually only very few systems included in this database offer this information, a total of five systems for β_{eff} and two for Λ_{eff}. These are Orsphere (β_{eff}, Λ_{eff}, α), BFS1-73 (β_{eff}), IPEN/MB-01 (β_{eff}, Λ_{eff}), SNEAK-7A (β_{eff}) and SNEAK-7B (β_{eff}). Hence, an extensive bibliographic search has been carried out in the ICSBEP [NEA 2020a] and the literature (e.g. [Okajima 2002]). Results are summarized in Table 11 and fully included in Annex 1.

Once these systems have been identified, the SUMMON code [Romojaro 2017, Romojaro 2019] has been used in combination with sensitivity profiles calculated with the KSEN card of MCNP 6.2 [Werner 2017] in order to determine the sensitivity of β_{eff} and Λ_{eff} to nuclear data and the uncertainty due to nuclear data. The covariance matrices from the JEFF-3.3 [Plompen 2020], ENDF/B-VIII.0 [Brown 2018] and JENDL-4.0u [Shibata 2011] have been used for this purpose. This is tool offers similar S/U capabilities that the NDAST tool above mentioned and also makes use of the "sandwich rule" to calculate the uncertainty from the sensitivity profiles and covariance matrices, but it can perform S/U analyses in a more automatic way.

Table 11. Total number of benchmark systems with kinetic information identified within this work.

Fuel	Spectrum	β_{eff}	Λ_{eff}	α
^{235}U systems	Fast & intermediate	13	3	14
	Thermal	2	1	8
Pu & mixed fuel systems	Fast & intermediate	10	1	1
	Thermal	---	---	---
^{233}U systems	Fast & intermediate	2	1	1
	Thermal	---	---	---
	Total	27	6	24

4.2. Benchmarks for the effective delayed neutron fraction (β_{eff})

The effective delayed neutron fraction has been calculated with SUMMON using the technique proposed in [Chiba 2009, Chiba 2011]:

$$\beta_{eff} = \frac{1}{a}\left(\frac{\bar{k}_{eff}}{k_{eff}} - 1\right)$$

where k_{eff} is the criticality constant of the system and $\bar{k}_{eff}$ is the value of the criticality constant obtained by perturbing the system by introducing a times the number of delayed neutrons. This is achieved by multiplying by $a+1$ the value of the average number of delayed neutron per fission ($\bar{\nu}_d$) in the nuclear data files used by the Monte Carlo code and increasing accordingly the total number of neutrons per fission ($\bar{\nu}_t$). The results presented in this work have been obtained considering $a = 20$, which has been found to offer a good balance between precision and accuracy.

Major conclusions from the analysis are:

1) Experimental and calculated β_{eff} values are largely compatible when uncertainties due to nuclear data are taken into account.

2) Calculated values of β_{eff} are sensitive mostly to $\bar{\nu}_d$ (strong positive sensitivity, ISC ≅ 1) and $\bar{\nu}_p$ (strong negative sensitivity, ISC ≅ -1) of the major fissile isotopes. Some examples are presented in Table 12. Hence, β_{eff} is a good parameter for validating these data. This can be explained from the definition of β_{eff} in perturbation theory:

$$\beta_{eff} = \frac{\langle \psi^\dagger | \hat{F}_d \psi \rangle}{\langle \psi^\dagger | \hat{F} \psi \rangle} \simeq \frac{\langle \psi^\dagger | \hat{F}_d \psi \rangle}{\langle \psi^\dagger | \hat{F}_p \psi \rangle} = \frac{\langle \psi^\dagger | \chi_d \bar{\nu}_d \Sigma_f \psi \rangle}{\langle \psi^\dagger | \chi_p \bar{\nu}_p \Sigma_f \psi \rangle}$$

   From this equation it is straightforward that an increase in the value of $\bar{\nu}_d$ (in the numerator) will cause a proportional increase in the value of β_{eff} while an increase in $\bar{\nu}_p$ (in the denominator) will cause a proportional decrease in the value of β_{eff}. Notice that with this explanation a negative sensitivity to $\bar{\nu}$ could be also expected, but it is not observed. This is possibly due to the procedures used by MCNP to calculate the sensitivity profiles, e.g. because of not considering $\bar{\nu}$ when both $\bar{\nu}_p$ and $\bar{\nu}_d$ are available, but we have found no information about this in the literature. In any case, a similar behaviour was observed in [Kodeli 2013] with the SUS3D code.

3) Concerning uncertainties due to nuclear data, it has been observed a large variation in the uncertainty values obtained when using covariance data sets from different nuclear data libraries. The total uncertainty due to nuclear data and the major contributors for some systems are presented in Table 14, using covariance matrices from the JEFF-3.3, ENDF/B-VIII.0 and JENDL-4.0u libraries. The reason for the discrepancy between libraries is the inclusion or not of covariance information for the most relevant nuclear data for β_{eff}, i.e. $\bar{\nu}_d$ and $\bar{\nu}_p$. In Table 13, the isotopes with covariance data for nubar included in different libraries are listed. The most complete library in this sense is JENDL-4.0u. The ENDF/B-VIII.0 is also suitable for uncertainty analyses of uranium systems (both ^{233}U and ^{235}U), and in fact is more conservative (larger uncertainties) than JENDL-4.0u for ^{235}U systems. The JEFF-3.3 library, for its part, is only suitable for ^{233}U systems. In this case, however, it is the most conservative library.

   Another point to remark is that the uncertainty due to nuclear data is dominated by the uncertainty in $\bar{\nu}_d$. In spite of a similarly large sensitivity, $\bar{\nu}_p$ does not contribute significantly to this uncertainty. This is explained by lower covariance values in $\bar{\nu}_p$. Finally, in a few systems (Topsy, Sneak7B) the contribution of ^{238}U inelastic scattering is also very relevant or even the dominant one. This is consistent with the findings of previous works [Kodeli 2011, Kodeli 2013, Kodeli 2014, Kodeli 2017a, Kodeli 2017b].

Table 12. Integrated sensitivity coefficients (ISCs) to β_{eff} for selected systems.

Godiva (HEU-MET-FAST-001)	
Reaction	ISC (%/%)
^{235}U, $\bar{\nu}_d$	0.9698 ± 0.0016
^{235}U, (n,n)	0.050 ± 0.014
^{238}U, $\bar{\nu}_d$	0.02035 ± 0.00003
^{238}U, (n,f)	0.00682 ± 0.00011
^{234}U, $\bar{\nu}_d$	0.004650 ± 0.000007
…	
^{234}U, $\bar{\nu}_p$	-0.01254 ± 0.00007
^{238}U, $\bar{\nu}_p$	-0.01624 ± 0.00008
^{235}U, (n,γ)	-0.0458 ± 0.0009
^{235}U, (n,f)	-0.054 ± 0.012
^{235}U, $\bar{\nu}_p$	-0.966 ± 0.010

Jezebel (PU-MET-FAST-001)	
Reaction	ISC (%/%)
^{239}Pu, $\bar{\nu}_d$	0.9483 ± 0.0007
^{239}Pu, (n,n)	0.082 ± 0.010
^{240}Pu, $\bar{\nu}_d$	0.04218 ± 0.00003
^{241}Pu, $\bar{\nu}_d$	0.006865 ± 0.000006
^{240}Pu, (n,n)	0.0048 ± 0.0024
…	
^{240}Pu, $\bar{\nu}$	-0.0067 ± 0.0003
^{239}Pu, (n,f)	-0.013 ± 0.012
^{239}Pu, (n,γ)	-0.0206 ± 0.0003
^{240}Pu, $\bar{\nu}_p$	-0.0489 ± 0.0003
^{239}Pu, $\bar{\nu}_p$	-0.946 ± 0.011

Skidoo (U233-MET-FAST-001)	
Reaction	ISC (%/%)
^{233}U, $\bar{\nu}_d$	0.9824 ± 0.0016
^{233}U, (n,n)	0.064 ± 0.020
^{234}U, $\bar{\nu}_d$	0.00947 ± 0.00001
^{238}U, $\bar{\nu}_d$	0.00472 ± 0.00001
^{238}U, (n,f)	0.00336 ± 0.00002
…	
^{233}U, (n,n')	-0.010 ± 0.008
^{234}U, $\bar{\nu}_p$	-0.01141 ± 0.00012
^{233}U, (n,γ)	-0.0211 ± 0.0006
^{233}U, (n,f)	-0.066 ± 0.022
^{233}U, $\bar{\nu}_p$	-0.984 ± 0.020

Table 13. Covariance data for nubar in different nuclear data libraries.

	JEFF-3.3	ENDF/B-VIII.0	JENDL-4.0u
^{233}U	$\bar{\nu}$, $\bar{\nu}_d$, $\bar{\nu}_p$	$\bar{\nu}$, $\bar{\nu}_d$, $\bar{\nu}_p$	$\bar{\nu}$, $\bar{\nu}_d$, $\bar{\nu}_p$
^{234}U	$\bar{\nu}_p$	$\bar{\nu}_p$	$\bar{\nu}$, $\bar{\nu}_d$, $\bar{\nu}_p$
^{235}U	$\bar{\nu}_p$	$\bar{\nu}$, $\bar{\nu}_d$, $\bar{\nu}_p$	$\bar{\nu}$, $\bar{\nu}_d$, $\bar{\nu}_p$
^{238}U	$\bar{\nu}_p$	$\bar{\nu}$, $\bar{\nu}_d$, $\bar{\nu}_p$	$\bar{\nu}$, $\bar{\nu}_d$, $\bar{\nu}_p$
^{239}Pu	$\bar{\nu}_p$	$\bar{\nu}$, $\bar{\nu}_p$	$\bar{\nu}$, $\bar{\nu}_d$, $\bar{\nu}_p$
^{240}Pu	---	$\bar{\nu}_p$	$\bar{\nu}$, $\bar{\nu}_d$, $\bar{\nu}_p$
^{241}Pu	$\bar{\nu}$, $\bar{\nu}_d$, $\bar{\nu}_p$	$\bar{\nu}_p$	$\bar{\nu}$, $\bar{\nu}_d$, $\bar{\nu}_p$
^{242}Pu	---	$\bar{\nu}$, $\bar{\nu}_d$, $\bar{\nu}_p$	$\bar{\nu}$, $\bar{\nu}_d$, $\bar{\nu}_p$

Table 14. Uncertainty in β_{eff} for selected systems with different covariance data sets.

Godiva (HEU-MET-FAST-001)

JEFF-3.3				
Reaction				$\Delta\beta_{eff}/\beta_{eff}$ (%)
^{235}U	χ	^{235}U	χ	0.918 ± 0.021
^{235}U	(n,f)	^{235}U	(n,f)	0.839 ± 0.006
^{235}U	$\bar{\nu}$	^{235}U	$\bar{\nu}$	0.4717 ± 0.0015
^{235}U	(n,γ)	^{235}U	(n,γ)	0.3879 ± 0.0022
^{235}U	(n,n')	^{235}U	(n,f)	0.3570 ± 0.0024
^{235}U	(n,f)	^{235}U	(n,γ)	-0.2759 ± 0.0013
TOTAL				1.416 ± 0.014

ENDF/B-VIII.0				
Reaction				$\Delta\beta_{eff}/\beta_{eff}$ (%)
^{235}U	$\bar{\nu}_d$	^{235}U	$\bar{\nu}_d$	4.5580 ± 0.0021
^{235}U	$\bar{\nu}_p$	^{235}U	$\bar{\nu}_p$	0.4005 ± 0.0012
^{235}U	(n,γ)	^{235}U	(n,γ)	0.2534 ± 0.0015
^{235}U	(n,n')	^{235}U	(n,f)	-0.1799 ± 0.0024
^{235}U	$\bar{\nu}_d$	^{235}U	$\bar{\nu}_d$	0.15026 ± 0.00007
^{235}U	(n,n)	^{235}U	(n,n)	0.129 ± 0.008
TOTAL				4.5907 ± 0.0021

JENDL-4.0u				
Reaction				$\Delta\beta_{eff}/\beta_{eff}$ (%)
^{235}U	$\bar{\nu}_d$	^{235}U	$\bar{\nu}_d$	2.7300 ± 0.0013
^{235}U	χ	^{235}U	χ	0.594 ± 0.013
^{235}U	(n,n)	^{235}U	(n,n)	0.487 ± 0.020
^{235}U	(n,n')	^{235}U	(n,n')	0.445 ± 0.017
^{235}U	$\bar{\nu}_p$	^{235}U	$\bar{\nu}_p$	0.3824 ± 0.0008
^{235}U	$\bar{\nu}$	^{235}U	$\bar{\nu}_p$	0.3507 ± 0.0009
TOTAL				2.943 ± 0.005

Jezebel (PU-MET-FAST-001)

JEFF-3.3				
Reaction				$\Delta\beta_{eff}/\beta_{eff}$ (%)
^{239}Pu	χ	^{239}Pu	χ	0.699 ± 0.022
^{239}Pu	$\bar{\nu}_p$	^{239}Pu	$\bar{\nu}_p$	0.3673 ± 0.0015
^{239}Pu	(n,f)	^{239}Pu	(n,f)	0.1589 ± 0.0011
^{239}Pu	(n,n)	^{239}Pu	(n,f)	-0.1326 ± 0.0025
^{239}Pu	(n,f)	^{239}Pu	(n,γ)	0.1199 ± 0.0005
^{239}Pu	(n,n)	^{239}Pu	(n,γ)	-0.1194 ± 0.0005
TOTAL				0.806 ± 0.019

ENDF/B-VIII.0				
Reaction				$\Delta\beta_{eff}/\beta_{eff}$ (%)
^{239}Pu	(n,n)	^{239}Pu	(n,n')	-0.58 ± 0.04
^{239}Pu	(n,n)	^{239}Pu	(n,n)	0.476 ± 0.018
^{239}Pu	$\bar{\nu}_p$	^{239}Pu	$\bar{\nu}_p$	0.4753 ± 0.0012
^{239}Pu	(n,n')	^{239}Pu	(n,n')	0.401 ± 0.027
^{239}Pu	χ	^{239}Pu	χ	0.286 ± 0.007
^{239}Pu	$\bar{\nu}$	^{239}Pu	$\bar{\nu}$	0.2481 ± 0.0010
TOTAL				0.689 ± 0.022

JENDL-4.0u				
Reaction				$\Delta\beta_{eff}/\beta_{eff}$ (%)
^{239}Pu	$\bar{\nu}_d$	^{239}Pu	$\bar{\nu}_d$	2.2735 ± 0.0006
^{239}Pu	(n,n)	^{239}Pu	(n,n)	0.356 ± 0.010
^{239}Pu	$\bar{\nu}_p$	^{239}Pu	$\bar{\nu}_p$	0.3499 ± 0.0008
^{239}Pu	$\bar{\nu}$	^{239}Pu	$\bar{\nu}_p$	0.3469 ± 0.0008
^{239}Pu	χ	^{239}Pu	χ	0.316 ± 0.010
^{239}Pu	(n,f)	^{239}Pu	(n,f)	0.2063 ± 0.0009
TOTAL				2.4095 ± 0.0021

Skidoo (U233-MET-FAST-001)

JEFF-3.3				
Reaction				$\Delta\beta_{eff}/\beta_{eff}$ (%)
^{233}U	$\bar{\nu}_d$	^{233}U	$\bar{\nu}_d$	9.191 ± 0.005
^{233}U	χ	^{233}U	χ	0.677 ± 0.023
^{233}U	(n,γ)	^{233}U	(n,γ)	0.2889 ± 0.0021
^{233}U	$\bar{\nu}_p$	^{233}U	$\bar{\nu}_d$	0.27426 ± 0.00015
^{233}U	(n,n)	^{233}U	(n,n)	0.269 ± 0.013
^{233}U	$\bar{\nu}_p$	^{233}U	$\bar{\nu}_p$	0.2220 ± 0.0013
TOTAL				9.235 ± 0.005

ENDF/B-VIII.0				
Reaction				$\Delta\beta_{eff}/\beta_{eff}$ (%)
^{233}U	$\bar{\nu}_d$	^{233}U	$\bar{\nu}_d$	7.246 ± 0.004
^{233}U	$\bar{\nu}_p$	^{233}U	$\bar{\nu}_p$	0.842 ± 0.004
^{233}U	$\bar{\nu}$	^{233}U	$\bar{\nu}$	0.828 ± 0.004
^{233}U	χ	^{233}U	χ	0.677 ± 0.023
^{233}U	(n,n)	^{233}U	(n,n)	0.494 ± 0.022
^{233}U	$\bar{\nu}$	^{233}U	$\bar{\nu}$	0.480 ± 0.003
TOTAL				7.427 ± 0.005

JENDL-4.0u				
Reaction				$\Delta\beta_{eff}/\beta_{eff}$ (%)
^{233}U	$\bar{\nu}_d$	^{233}U	$\bar{\nu}_d$	7.246 ± 0.004
^{233}U	$\bar{\nu}_p$	^{233}U	$\bar{\nu}_p$	0.842 ± 0.004
^{233}U	$\bar{\nu}$	^{233}U	$\bar{\nu}_p$	0.828 ± 0.004
^{233}U	χ	^{233}U	χ	0.677 ± 0.023
^{233}U	(n,n)	^{233}U	(n,n)	0.494 ± 0.022
^{233}U	$\bar{\nu}$	^{233}U	$\bar{\nu}$	0.480 ± 0.003
TOTAL				7.429 ± 0.005

4.3. Benchmarks for the mean neutron generation time (Λ_{eff})

SUMMON calculates Λ_{eff} and its sensitivity profiles with the technique described in [Verboomen 2006]. With this technique, the system is perturbed by introducing a homogeneous atomic concentration N of an isotope with a capture cross section of the shape A/v. Applying perturbation theory, the following relationship between the reactivity difference due to the perturbation and Λ_{eff} can be obtained:

$$\rho - \rho_0 = -N \cdot A \cdot \Lambda_{eff} \Rightarrow \Lambda_{eff} = -\frac{\rho - \rho_0}{N \cdot A}$$

where ρ and ρ_0 are, respectively, the perturbed and reference (unperturbed) values of the reactivity of the system.

As stated above, experimental data for Λ_{eff} are much more scarcer than for β_{eff}, only six systems having been identified. The Rossi-α ($\alpha = -\beta_{eff}/\Lambda_{eff}$) is more commonly found in the literature (24 systems) and hence may be more suitable for nuclear data validation, but it is beyond its work. Nevertheless, some general conclusions can be extracted:

1) The agreement between experimental and calculated data is somewhat worse than for the case of β_{eff}. However, the much larger range of variation of Λ_{eff} than of β_{eff} has to be taken into account.
2) A strong, negative sensitivity (about -1) of Λ_{eff} to several fission-related data ((n,f), $\bar{\nu}$, $\bar{\nu}_p$) is observed for all systems analysed, both fast and thermal. Some examples are presented in Table 15. This can be explained from the presence of the fission operator $\hat{F}$ in the denominator of the definition of Λ_{eff} in perturbation theory:

   $$\Lambda_{eff} = \frac{\langle \psi^\dagger | \frac{1}{v} \psi \rangle}{\langle \psi^\dagger | \hat{F} \psi \rangle}$$

   On the other hand, because of the expression in the numerator, a decrease in the neutron energy (i.e. in v) should result in an increase of the value of Λ_{eff}. This explains the observed positive sensitivity to scattering reactions in the case of fast systems. Interestingly enough, in the case of the sole thermal system in the analysis (MB-01) the sensitivity to the $^{1}\mathrm{H}$ (n,n) reaction is actually negative.
3) The uncertainty due to nuclear data in Λ_{eff} is about 2-3% for fast systems while for the only thermal system studied is less than 1%. Results for the JEFF-3.3 library are presented in Table 16. The total uncertainty values are similar for the ENDF/B-VIII.0 and JENDL-4.0u libraries, although significant differences between libraries concerning individual reactions have been observed. However, no general trend has been identified.

Table 15. Λ_{eff} integrated sensitivity coefficients (ISCs) to for selected systems.

Orsphere (HEU-MET-FAST-001)	
Reaction	ISC (%/%)
^{235}U, (n,n)	0.26 ± 0.08
^{235}U, (n,n')	0.20 ± 0.04
^{238}U, (n,n)	0.012 ± 0.020
^{238}U, (n,n')	0.011 ± 0.012
^{234}U, (n,n')	0.009 ± 0.004
…	
^{238}U, $\bar{\nu}$	-0.0165 ± 0.0010
^{235}U, (n,γ)	-0.081 ± 0.005
^{235}U, $\bar{\nu}_p$	-0.97 ± 0.06
^{235}U, $\bar{\nu}$	-0.97 ± 0.06
^{235}U, (n,f)	-1.11 ± 0.07

FR0-5 (IEU-MET-FAST-022)	
Reaction	ISC (%/%)
^{1}H, (n,n)	0.238 ± 0.005
^{238}U, (n,n')	0.087 ± 0.003
^{63}Cu, (n,n)	0.037 ± 0.007
^{65}Cu, (n,n)	0.021 ± 0.005
^{235}U, (n,n')	0.0193 ± 0.0015
…	
^{238}U, $\bar{\nu}_p$	-0.2853 ± 0.0011
^{238}U, $\bar{\nu}$	-0.2893 ± 0.0011
^{235}U, $\bar{\nu}_p$	-0.704 ± 0.004
^{235}U, $\bar{\nu}$	-0.707 ± 0.004
^{235}U, (n,f)	-1.051 ± 0.004

MB-01 (LEU-COMP-THERM-077)	
Reaction	ISC (%/%)
^{238}U, (n,γ)	0.0755 ± 0.0005
^{235}U, (n,γ)	0.0334 ± 0.0003
^{16}O, (n,α)	0.001784 ± 0.000026
^{109}Ag, (n,γ)	0.00153 ± 0.00007
^{115}In, (n,γ)	0.00102 ± 0.00006
…	
^{1}H, (n,γ)	-0.1059 ± 0.0005
^{1}H, (n,n)	-0.265 ± 0.009
^{235}U, (n,f)	-0.8171 ± 0.0028
^{235}U, $\bar{\nu}_p$	-0.9064 ± 0.0023
^{235}U, $\bar{\nu}$	-0.9129 ± 0.0023

Table 16. Uncertainty in Λ_{eff} due to nuclear data. JEFF-3.3 covariance matrices.

Orsphere (HEU-MET-FAST-100)				
Reaction				$\Delta\Lambda_{eff}/\Lambda_{eff}$ (%)
^{235}U	(n,n')	^{235}U	(n,n')	2.0 ± 0.4
^{235}U	χ	^{235}U	χ	1.6 ± 0.4
^{235}U	(n,n')	^{235}U	(n,f)	-1.2 ± 0.4
^{235}U	(n,n')	^{235}U	(n,γ)	-1.05 ± 0.06
^{235}U	(n,f)	^{235}U	(n,f)	0.94 ± 0.09
^{235}U	(n,γ)	^{235}U	(n,γ)	0.68 ± 0.04
^{235}U	(n,f)	^{235}U	(n,γ)	-0.63 ± 0.04
^{235}U	(n,n)	^{235}U	(n,n')	-0.60 ± 0.12
^{235}U	$\bar{\nu}$	^{235}U	$\bar{\nu}$	0.48 ± 0.03
^{235}U	(n,n)	^{235}U	(n,f)	0.38 ± 0.08
TOTAL				2.3 ± 0.4

FR0-5 (IEU-MET-FAST-022)				
Reaction				$\Delta\Lambda_{eff}/\Lambda_{eff}$ (%)
^{235}U	(n,f)	^{235}U	(n,f)	1.95 ± 0.06
^{235}U	χ	^{235}U	χ	1.05 ± 0.19
^{238}U	(n,f)	^{238}U	(n,f)	0.67 ± 0.03
^{238}U	(n,n')	^{238}U	(n,f)	-0.568 ± 0.025
^{235}U	(n,γ)	^{235}U	(n,γ)	0.555 ± 0.015
^{235}U	(n,f)	^{235}U	(n,γ)	0.50 ± 0.05
^{238}U	(n,n')	^{238}U	(n,n')	0.38 ± 0.19
^{235}U	$\bar{\nu}_p$	^{235}U	$\bar{\nu}_p$	0.368 ± 0.016
^{238}U	$\bar{\nu}_p$	^{238}U	$\bar{\nu}_p$	0.281 ± 0.008
^{235}U	(n,n')	^{235}U	(n,f)	-0.247 ± 0.012
TOTAL				2.47 ± 0.10

MB-01 (LEU-COMP-THERM-077)				
Reaction				$\Delta\Lambda_{eff}/\Lambda_{eff}$ (%)
^{235}U	(n,f)	^{235}U	(n,f)	0.5470 ± 0.0019
^{235}U	$\bar{\nu}_p$	^{235}U	$\bar{\nu}_p$	0.5080 ± 0.0013
^{1}H	(n,γ)	^{1}H	(n,γ)	0.2703 ± 0.0012
^{1}H	(n,n)	^{1}H	(n,n)	0.209 ± 0.005
^{238}U	(n,f)	^{238}U	(n,f)	0.2078 ± 0.0017
^{238}U	(n,n')	^{238}U	(n,f)	0.1843 ± 0.015
^{16}O	(n,n)	^{16}O	(n,n)	0.154 ± 0.011
^{235}U	χ	^{235}U	χ	0.150 ± 0.016
^{238}U	(n,n')	^{238}U	(n,n')	0.121 ± 0.008
^{238}U	(n,n)	^{238}U	(n,f)	0.0899 ± 0.0008
TOTAL				0.922 ± 0.004

4.4. Recommendations

The results of the review of the databases and the literature for reactor kinetics benchmark experiments allow us to make the following recommendations:

- A relatively small number of benchmark systems with kinetic parameter information is available. Hence, a review of the documentation about former reactor kinetics experiments that may be conserved in institutions which operate or have previously operated research nuclear reactors is recommended.
- β_{eff} is well suited for the validation of $\bar{\nu}_d$ and $\bar{\nu}_p$ data due to its high sensitivity to these data.
- Λ_{eff}, for its part, is well suited for validating fission-related data ((n,f), $\bar{\nu}$, $\bar{\nu}_p$), and, to a lesser extent, scattering data.
- Experimental values for the Rossi-α ($\alpha = -\beta_{eff}/\Lambda_{eff}$) are more commonly found in the literature than experimental values for Λ_{eff} and can also be used for nuclear data validation.

4.5. References

[Bécares 2022] V. Bécares *et al.*, *Review of available benchmark experiments for kinetic parameter validation*. CIEMAT report DFN/IN-04/II-22. Issued on 13 October 2022.

[Brown 2018] D. A. Brown *et al.*, *ENDF/B-VIII.0: The 8th Major Release of the Nuclear Reaction Data Library with CIELO-project Cross Sections, New Standards and Thermal Scattering Data*. Nuclear Data Sheets 148 (2018) 1-142.

[Chiba 2009] G. Chiba, *Calculation of Effective Delayed Neutron Fraction Using a Modified k-Ratio Method*. Journal of Nuclear Science and Technology 46 (2009) 399-402. DOI: 10.1080/18811248.2007.9711546.

[Chiba 2011] G. Chiba *et al.*, *JENDL-4.0 Benchmarking for Effective Delayed Neutron Fraction of Fast Neutron Systems*. Journal of Nuclear Science and Technology 48 (2011) 1471–1477. DOI: 10.1080/18811248.2011. 9711840.

[Kodeli 2011] I. Kodeli, *Sensitivity and uncertainty in the effective delayed neutron fraction β$_{eff}$ (method and SNEAK-7A example)*, proc. UAM-5 Workshop, Stockholm, Apr. 13-15, 2011, OECD/NEA.

[Kodeli 2013] I. Kodeli, *Sensitivity and uncertainty in the effective delayed neutron fraction (β$_{eff}$)*. Nucl. Instrum. Methods Phys. Res. A 715 (2013) 70–78. DOI: 10.1016/j.nima.2013.03.020.

[Kodeli 2014] I. Kodeli and W. Zwermann, *Evaluation of Uncertainties in β$_{eff}$ by Means of Deterministic and Monte Carlo Methods*. Nuclear Data Sheets 118 (2014) 370–373. DOI: 10.1016/j.nds.2014.04.083.

[Kodeli 2017a] I. Kodeli *et al.*, *Study of Uncertainty in Kinetic Parameters in the Scope of the UAM-SFR Project of OECD*. In 26th International conference Nuclear Energy for New Europe (NENE 2017) Bled (Slovenia) 11-14 September 2017.

[Kodeli 2017b] I. Kodeli *et al.*, *Uncertainty Analysis of Kinetic Parameters for Design, Operation and Safety Analysis of SFRs*, Proc. Int. Conf. on Fast Reactors and Related Fuel Cycles: Next Generation Nuclear Systems for Sustainable Development (FR17), Yekaterinburg (Russian Federation) 26-29 June 2017.

[NEA 2020a] ICSBEP Handbook 2020, *International Criticality Safety Benchmark Evaluation Project Handbook* (database). DOI: 10.1787/7e0ebc50-en (accessed on 05 September 2022).

[NEA 2020b] IRPhE Handbook 2020, *International Reactor Physics Evaluation Project Handbook* (database). DOI: 10.1787/d863e360-en (accessed on 05 September 2022).

[Okajima 2002] S. Okajima *et al.*, *Summary on International Benchmark Experiments for Effective Delayed Neutron Fraction* (β$_{eff}$), Progress in Nuclear Energy 41 (2002) 285-301.

[Plompen 2020] A. J. M. Plompen *et al.*, *The joint evaluated fission and fusion nuclear data library, JEFF-3.3*. European Physical Journal A 56 (2020) 181. DOI: 10.1140/epja/s10050-020-00141-9.

[Romojaro 2017] P. Romojaro *et al.*, *SUMMON: A Sensitivity And Uncertainty Methodology For MONte Carlo Codes*. Proceedings of International Conference on Mathematics & Computational Methods Applied to Nuclear Science & Engineering (M&C 2017), Jeju (Korea) 16-20 April 2017.

[Romojaro 2019] P. Romojaro *et al.*, *Sensitivity methods for effective delayed neutron fraction and neutron generation time with summon*. Annals of Nuclear Energy 126 (2019) 410–418. DOI: 10.1016/j.anucene.2018.11.042.

[Verboomen 2006] B. Verboomen *et al.*, *Monte Carlo calculation of the effective neutron generation time.* Annals of Nuclear Energy 33 (2006) 911-916.

[Werner 2017] C. J. Werner (Ed.), *MCNP User's Manual. Code Version 6.2*. Los Alamos National Laboratory Report LA-UR-17-29981 (2017).

5. Fuel depletion benchmarks

The database SFCOMPO (Spent Fuel Isotopic Composition), released and maintained by OECD/NEA, includes experimental assay data of spent nuclear fuel. These are mostly limited to nuclide composition data in combination with corresponding reactor operational histories and design data. The current version, SFCOMPO-2.0 [Michel-Sendis 2017], was publicly released in June 2017.

The SFCOMPO database generally includes some important components of the nuclide vector, mostly measured using destructive radiochemical analysis of samples consisting of segments of irradiated fuel rods of different types of reactors. Within the OECD/NEA WPNCS (Working Party on Nuclear Criticality Safety) SFCOMPO TRG (Technical Review Group), there is currently an effort underway to include experimental data on decay heat.

In addition to cases present in the SFCOMPO-2.0 database, other experiments with spent nuclear fuel exist. For many cases of spent PWR and BWR fuel, decay heat was measured using the calorimeter located at the interim spent fuel storage facility CLAB in Sweden [CLAB 2006].

5.1. Overview of the SFCOMPO-2.0 database

The SFCOMPO database comprises information about fuel samples (measured within the past 50 years) irradiated in different types of power reactors:

- PWR (308 samples from 16 reactors)
- VVER (67 samples from 7 reactors)
- BWR (249 samples from 12 reactors)
- CANDU (31 samples from 3 reactors)
- AGR (63 samples from 3 reactors)
- MAGNOX (4 samples from 2 reactors)
- RBMK (41 samples from 1 reactor)

Obviously, the reactor design data, which include the information about the material composition and geometry of fuel, moderator, cladding and possibly other components, primarily depends on the type of the reactor. However, for a given reactor type, the detailed design affects the final spent fuel composition. For example, for PWR, the following design parameters are important for the spent fuel composition [Romojaro 2022]:

- Initial fuel composition:
  - UO_2:
    - ^{235}U enrichment: affects reactivity and build-up of all actinides and to lesser extent fission products (in SFCOMPO: from 1.6874 wt.% to 4.66 wt.%).
    - ^{236}U contamination: primarily affects build-up of ^{237}Np and ^{238}Pu (in SFCOMPO: up to 0.033 wt.%, often not given).
    - Burnable absorbers: affects reactivity gradient with respect to burnup and neutron spectrum and local power distribution (in SFCOMPO: 14 or 16 fuel rods containing Gd_2O_3 within 17 × 17 fuel assemblies).
  - MOX:
    - Pu content: affects build-up of heavier actinides (in SFCOMPO: from 5.5 wt.% to 6.011 wt.%).
    - $^{239,241}Pu$ enrichment: affects reactivity and build-up of heavier actinides (in SFCOMPO: from 70.506 wt.% to 72.64 wt.%).
- Fuel/moderator ratio: affects neutron spectrum which influences build-up of ^{239}Pu and other heavier actinides (in SFCOMPO: fractional fuel volumes in unit cell from 0.44 to 0.51).
- Soluble boron content in moderator: affects neutron spectrum which influences build-up of ^{239}Pu and other heavier actinides (in SFCOMPO: up to 1920 ppm).

- Fuel pellet radius (or equivalently, at a fixed fuel/moderator ratio, rod pitch): self-shielding causes rim effect which affects reactivity, radial burnup (BU) distribution and build-up of nuclides which have highly non-linear dependence on BU, such as e.g. ^{244}Cm (in SFCOMPO: from 0.4318 cm to 0.559 cm).
- Cladding composition: affects reactivity and in case of Co impurity also gamma-ray activity and decay heat (in SFCOMPO: Zircaloy-4, sn-Zircaloy-4, ZIRLO and SS-348).

In contrast to the design data, which solely rely on specifications and measurements, the operational history data to some extent rely on calculations and/or assumptions on nuclear data. The following parameters are important for the spent fuel composition [Romojaro 2022]:

- Burnup (BU): is approximately proportional to the total number of fissions per initial metal atom (FIMA) and directly affects build-up of all actinides and all long-lived and stable fission products (in SFCOMPO: from 3.4 GWd/t up to 75 GWd/t).
- Irradiation time (including detailed power history): at a given BU/FIMA it is important for build-up of short-lived nuclides (in SFCOMPO: from 215 d to 1970 d).
- Cooling time: it directly the content of all radioactive nuclides and some stable nuclides.
- Fuel and moderator temperatures: affects reactivity and build-up of all actinides and to lesser extent fission products (in SFCOMPO: in some cases, detailed information is given, in other cases assumptions need to be made based on power density, etc.).

The measured observables are nuclide compositions and some other derived quantities. In total, compositions of about 100 nuclides were determined mostly based on radiochemical analysis, and to part based on NDA techniques. The latter primarily include gamma-ray spectrometry, in the future neutron emission measurements are possible (e.g. to determine the ^{244}Cm content) [Schillebeeckx 2020]. In SFCOMPO, the following measured and derived quantities can be found:

- Activities and activity ratios.
- Nuclide compositions, number and mass ratios.
- Concentrations, fractions or masses of individual elements or several elements (e.g. U+Pu).
- “Depletion” (in terms of reduction of the nuclide concentration or mass).
- BU/FIMA.

The database thus offers a large variety of cases which enable comparison and validation of nuclear data. However, some general issues persist:

- The detailed power history given is typically derived using full-core calculations from thermal power data measured on the reactor core level. Lack of information on assumptions done in the calculations to obtain the detailed local power history may, due to the lack of uncertainty data, result in hidden biases.
- Similarly, (fuel and moderator) temperatures are rarely measured directly. When information on temperature profiles is given, it typically relies on calculations or simplified assumptions, which are often not stated explicitly.
- Normalisation of depletion calculations can typically be done in one of the two following ways:
    - To BU: all nuclide compositions depend on the possible bias and uncertainty (which is most of the time not given) in BU as well as in the recoverable energy per fission.
    - To a burnup indicator (BI) nuclide (e.g. ^{148}Nd) or a combination of BI nuclides: all nuclide compositions depend on biases and uncertainties in the given BI nuclide concentrations as well as in the BI nuclide fission yields and possible secondary production paths.

5.2. Computational analysis performed by JSI

5.2.1. GU3 sample, NPP Gösgen

Within the framework of the OECD/NEA WPNCS SG10, a C/E comparison was done for the GU3 sample from the PWR reactor from the Gösgen NPP in Switzerland. This case was chosen since the pin of the measured samples was moved to a different fuel assembly for the last cycle. The computational model was based on the benchmark proposed by the WPNCS SG7 report [Carmouze 2021] consisting of simplified irradiation history and design data. Some components of the nuclide vector obtained from Serpent calculations using ENDF/B-VII.1 library in comparison with experimental values are presented in Table 17. The results for the considered nuclides, normalised to measured ^{148}Nd content, are consistent with most other participants, and also with experimental data, with a few notable exceptions:

- ^{241,242m}Am: There is an inconsistency with capture cross sections for ^{242g}Am and ^{242m}Am between Serpent and ENDF/B-VII.1 library.
- ^{103}Rh: Problems with the experimental data?
- ^{234}U: Most probably an issue with provided initial fuel composition.
- ^{149}Sm: Possible issues with the Serpent model.

Table 17. Comparison of a part of the nuclide vector for the Gösgen NPP GU3 sample using Serpent model and ENDF/B-VII.1 nuclear data library.

Nuclide	C/E-1 / %	Uncertainty	
		Experimental / %	ND / %
^{234}U	38.1	0.01	
^{235}U	3.7	0.32	1.6
^{236}U	-0.3	0.31	1.2
^{238}U	-0.7	0.01	0.02
^{241}Am	13.7	0.79	1.7
^{242m}Am	-28.8	5.29	2.6
^{243}Am	7.1	1.74	8.4
^{237}Np	-11.7	3	2.9
^{238}Pu	6.1	0.28	4.2
^{239}Pu	-0.9	0.19	1.6
^{240}Pu	1.7	0.15	1.9
^{241}Pu	0.1	0.28	1.5
^{242}Pu	0.8	0.02	3.7
^{143}Nd	2.9	0.28	3
^{149}Sm	19.1	1.05	6
^{152}Sm	3.3	0.32	3
^{155}Gd	8.3	1	12
^{103}Rh	27.6	2.44	
^{133}Cs	2.8	0.94	0.6
^{134}Cs	0.1	1.44	4.1
^{137}Cs	1.9	0.52	0.7
^{90}Sr	4.0	0.32	
^{148}Nd	0.1	0.29	0.4
^{242}Cm	-2.4	2.02	2
^{244}Cm	-1.2	1.57	9.5

5.2.2. Samples from NPP Calvert Cliffs-1 rods NBD107, MKP109 and MLA098

Additionally, a C/E comparison for samples from NPP Calvert Cliffs-1 PWR reactor was performed. This NPP was chosen as its design is slightly unconventional with larger than usual guide tubes. Results for selected nuclides are presented in Table 18 - Table 20 and are consistent for stable (^{148}Nd) and long-lived (^{239}Pu) nuclides. For other nuclides major discrepancies are observed. Possible reasons include:

- Biases in measurement method primarily for ^{137}Cs, where gamma-ray spectrometry was used.
- Operational history inconsistences, mainly control rod movement and power distribution history, which could greatly affect the local ^{137}Cs content among other due to possible migration within the fuel pin. However, this seems to be less likely since the local burnup is within 0.3 % of measured value for all samples.
- Inconsistencies in cooling time before measurement, this would affect both ^{241}Am and ^{137}Cs although for sample Q in rod NBD107 ^{241}Am prediction is consistent with the measurement.
- Inconsistencies due to possible (unreported) Pu/Am chemical separation before the measurement. If this was done months before the mass spectroscopic measurement, it could significantly affect the measured ^{241}Am (and ^{241}Pu) content.
- Unknown errors in the Serpent model.

For samples from rod MLA098, predictions are consistent for all nuclides, which reduced the probability of the errors in the Serpent model, since modelled assemblies differ only by initial enrichment and operational history. Overall, the results are consistent for different nuclear data libraries.

Table 18. C/E of composition for selected nuclides in rod NBD107 (assembly BT03); samples GG, MM and Q.

ND library	ENDF/B-VII.1			ENDF/B-VIII.0			JEFF-3.1		
Nuclide\Sample	**GG**	**MM**	**Q**	**GG**	**MM**	**Q**	**GG**	**MM**	**Q**
^{148}Nd	-	-	-	-	-	-	-	-	-
^{137}Cs	0.81(4)	0.78(4)	0.78(4)	0.81(4)	0.78(4)	0.78(4)	0.82(4)	0.79(4)	0.78(4)
^{239}Pu	0.97(2)	0.98(2)	0.99(2)	0.97(2)	0.97(2)	0.99(2)	0.97(2)	0.98(2)	1.0(2)
^{241}Am	1.48(5)	1.67(5)	1.08(5)	1.48(5)	1.65(5)	1.07(5)	1.48(5)	1.66(5)	1.09(5)

Table 19. C/E of composition for selected nuclides in rod MKP109 (assembly D047); samples CC, LL and P.

ND library	ENDF/B-VII.1			ENDF/B-VIII.0			JEFF-3.1		
Nucl.\Sample	**CC**	**LL**	**P**	**CC**	**LL**	**P**	**CC**	**LL**	**P**
^{148}Nd	1.01(-)	1.01(-)	1.02(-)	1.02(-)	1.01(-)	1.02(-)	1.02(-)	1.02(-)	1.02(-)
^{137}Cs	0.83(4)	0.82(4)	0.82(4)	0.83(4)	0.82(4)	0.82(4)	0.83(4)	0.82(4)	0.82(4)
^{239}Pu	0.9973(2)	1.0000(2)	1.0100(2)	0.993(2)	0.990(2)	1.000(2)	1.0042(2)	1.000(2)	1.0100(2)
^{241}Am	1.73(5)	1.84(5)	1.72(5)	1.71(5)	1.81(5)	1.71(5)	1.72(5)	1.82(5)	1.71(5)

Table 20. C/E of composition for selected nuclides in rod MLA098 (assembly D101); samples CC, LL and P.

ND library	ENDF/B-VII.1			ENDF/B-VIII.0			JEFF3.1		
Nucl.\Sample	**BB**	**JJ**	**P**	**BB**	**JJ**	**P**	**BB**	**JJ**	**P**
^{148}Nd	-	-	-	-	-	-	-	-	-
^{137}Cs	0.97(4)	0.94(4)	0.98(4)	0.97(4)	0.97(4)	0.98(4)	0.98(4)	0.98(4)	0.98(4)
^{239}Pu	0.98(2)	0.98(2)	1.01(2)	0.97(2)	0.97(2)	1.01(2)	0.98(2)	0.98(2)	1.02(2)
^{241}Am	0.97(5)	1.13(5)	0.96(5)	0.96(5)	0.96(5)	0.95(5)	0.97(5)	0.96(5)	0.95(5)

5.3. Other fuel depletion experiments

In collaboration with SCK CEN, two neutron transport codes were validated using CLAB spent nuclear fuel decay heat (DH) rate measurements [CLAB 2006], for fuel assemblies irradiated in 1980's and 1990's. In particular, at JSI DH rates were predicted using Monte Carlo (MC) neutron transport code Serpent version 2.31 [Leppänen 2013] with ENDF/B-VII.1 nuclear data library. Aforementioned measurements include data from total of 66 different fuel assemblies from both PWR and BWR reactors, all measured at CLAB using calorimetric and gamma-ray scanning methods [CLAB 2006].

Operational history and assembly specifications were taken from CLAB [CLAB 2006] and US Nuclear regulatory commission [Nureg 2006] reports. With decay times ranging from 6500 days to 9000 days (i.e. 16 years to 25 years) and burnup from 30 GWd/t to 54 GWd/t. Calculations were done using 2D model with reflective boundary conditions and assembly averaged parameters. This was deemed sufficient enough in particular for PWR cases where coolant density, burnup and power distribution among other parameters remain roughly homogeneous in axial direction. Exception are the top and the bottom parts, which roughly account for 25 % of whole assembly. On the other hands, for BWR cases strong axial parameter variations are observed. In regard to this, axial volumetric average parameters were used in calculations, with possible uncertainties in calculated results due to this simplification in mind.

Results of the C/E comparison are presented in Figure 5 with regards to initial enrichment (ie) and burnup (BU). On average, a slight shift from over prediction at low ie to under prediction for higher ie is observed in BWR cases. This effect is not evident in PWR assemblies. This might be due to greater axial power gradients in higher enriched fuels mainly for BWR cases since the power is primarily controlled by control blades (which are not modelled due to insufficient data) and burnable absorbers which are not axially homogeneous. In PWR cases this might not be as pronounced due to usage of boric acid as primary absorber during operation, which is easily modelled since it is uniformly distributed in the moderator. Additionally, in BWR cases with higher initial enrichments less regulation is done with control blades and more with burnable absorbers (which are modelled). This is shown in Annex 4**.** Consequently, for higher enrichment cases operation is modelled more thoroughly thus lower C/E. As for burnup dependence, similar trend could be observed for higher burnups, with PWR cases being again less dependent on burnup and more evenly distributed around ideal prediction. For both reactor types, DH rate is on average overpredicted.

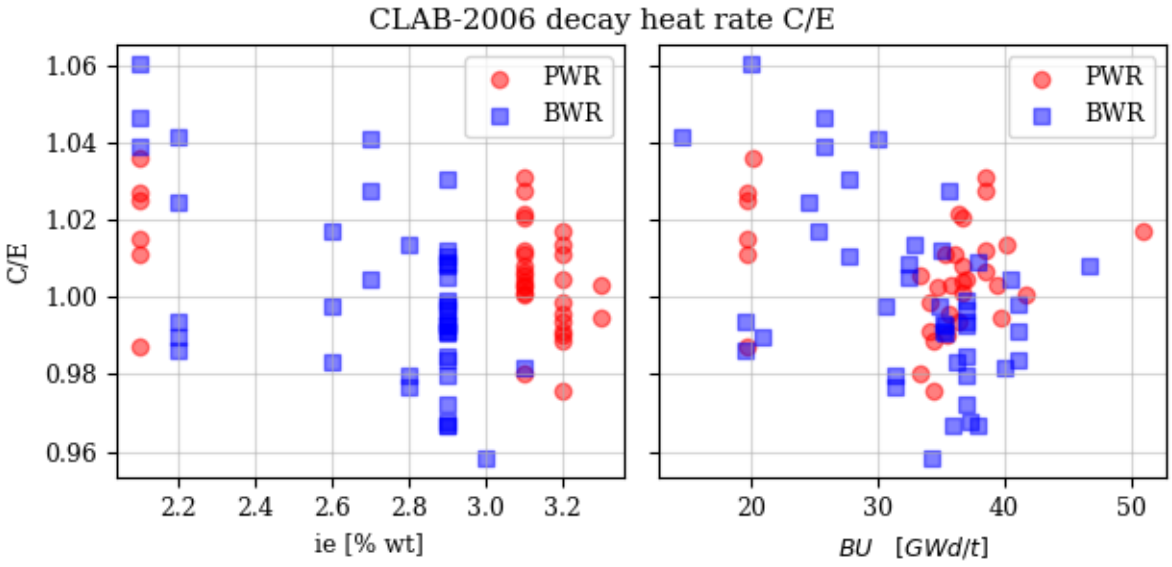

Figure 5. DH rate C/E for all measured fuel assemblies in relation to initial enrichment (ie) and burnup (BU).

During the simulation campaign, possible uncertainties due to abovementioned simplifications were estimated using so-called axial zoning, i.e. a simplified 3D model using 2D axial slices (in our case 25). Since such analysis was already conducted in the US Nuclear regulatory commission report [Nureg 2006] for calculations with

ORIGEN, we focused only on BWR cases where axial effects were shown to be of greater importance. Due to excessive computational time required calculations were done only for some cases. Those are presented in Figure 6, where it is evident that for cooling time in the range of DH rate measurements (i.e. 16 years to 25 years) one-zone model underpredicts the DH for around 1 % (10288 assembly), which could be compensated by defining weighted axial parameter average, mainly for the moderator density.

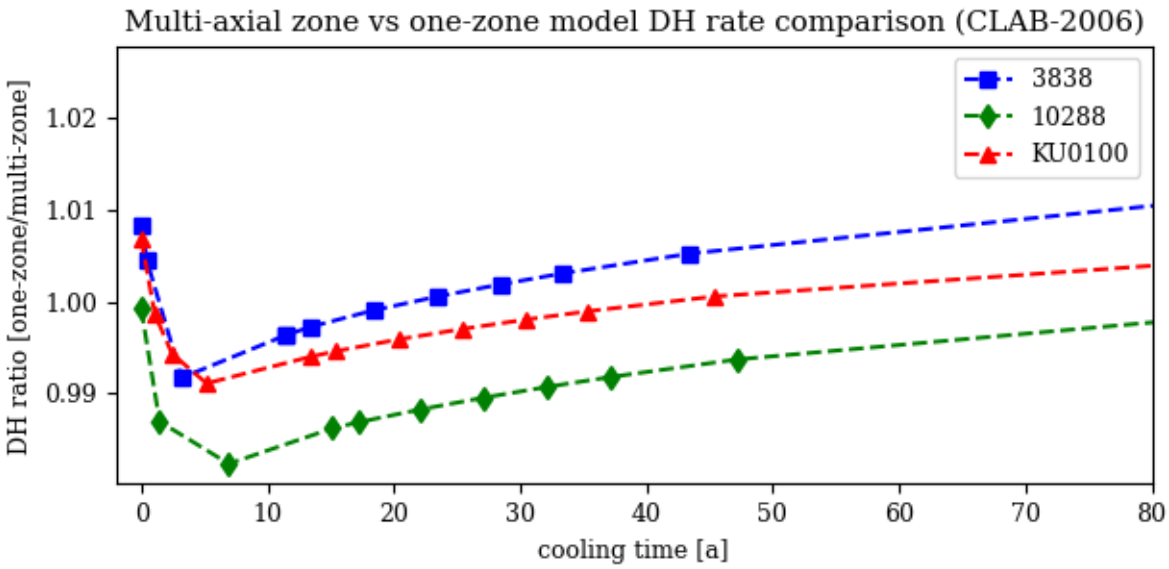

Figure 6. Ratio of DH rate calculated using assembly average parameters to explicit multi axial model (25 axial zones) calculations for selected BWR assemblies as a function of cooling time.

In addition, sensitivity to most important parameters was done and is presented in Figure 7. Burnup, which might vary for up to 5 % in the operational data, was shown to have greater effect on DH rate than the moderator density. Within the relevant cooling time range, DH rate sensitivity (*S* = change in DH rate [%]/ change in input parameter [%]) is slightly above 1. For moderator density, which in the 2D case varies only due to means of determining axial average from given axial distribution, the relative sensitivity is 4 times smaller by absolute value, but negative. Asymmetry in *S* due to direction of parameter change is also observed primarily with burnup variation.

A blind test on spent nuclear fuel was organised to compare the decay heat rates from 5 spent PWR fuel assemblies from previously unpublished measurements from the CLAB calorimeter [Jansson 2022]. JSI participated in this exercise with calculations using the computer codes Serpent and DRAGON using ENDF/B-VII.1. By comparison of the 5 assembly cases with results from other participating research groups it was concluded that the statistical spread from using different computer codes, modelling assumptions and nuclear data libraries is significantly smaller than the difference of the calculated means from the experimental values. From the available results, it is not possible to conclusively determine the origin of this difference. Hypotheses are: hidden biases in nuclear data, incomplete irradiation history data, experimental biases, or other unknown sources. Further investigation is needed to pinpoint the sources of bias and reduce the final uncertainties.

In order to address this issue, a more extensive blind exercise on decay heat, so-called SKB-50, which includes 50 cases of both PWR and BWR assemblies for which decay heat rate was more recently (compared to the CLAB 2006 cases) measured at the CLAB calorimeter, is planned for the near-term future. In parallel, work is being done on analysis and interpretation (including full uncertainty propagation) of the experimental data from the calorimeter.

Apart from the measurements at the CLAB calorimeter, a number of measurements, often using NDA techniques, with spent nuclear fuel were performed independently. As an example, neutron emission measurements using a spent fuel rod segment sample from Tihange NPP (PWR) were performed at SCK CEN and

JRC Geel [Schillebeeckx 2020]. JSI has been involved with depletion calculation and development of the methodology for interpretation of experimental data.

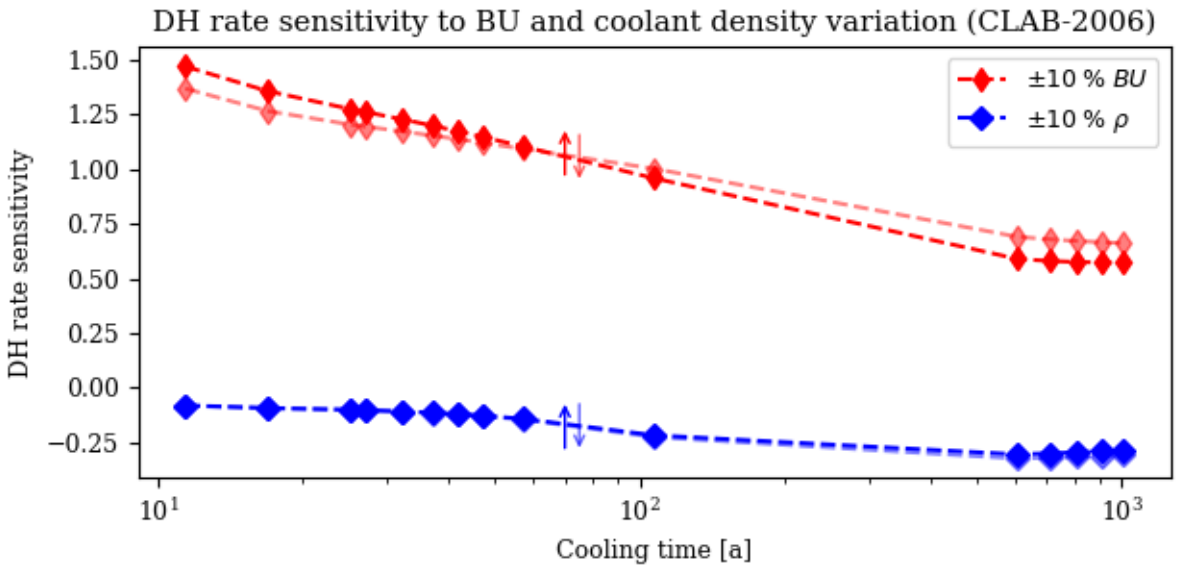

Figure 7. DH rate sensitivity S (S = change in DH rate [%]/ change in input parameter [%]) in relation to cooling time, for BWR 1177 (8 × 8) fuel assembly from Ringhals 1 NPP. *Bold and shaded lines indicate S for positive and negative change in input parameter respectively (also annotated by matching up and down arrows i.e. up arrow indicates sensitivity to positive change in input parameters)*.

5.4. Computational analysis performed by UPM: a pin-cell benchmark computational exercise to assess the reactivity change with burnup (*"the burnup issue"*).

Burnup is a complex issue which is related to the large underestimation of reactivity in LWR burnup calculations using recent nuclear data evaluations, JEFF-3.3 and ENDF/B-VIII.0. The aim of this work is to point out the main contributors of these reactivity changes [JEFDOC-2111, JEFF/BU, 2021]. This work has been performed using a simple "pin-cell" calculation for the analysis of reactivity change during burnup in LWRs. Table 21 shows a description of the pin-cell problem.

Calculations have been performed with the deterministic code WIMSD5b, using the WIMSD-69g library processed with NJOY code:

- JEFF-3.3 and ENDF/B-VIII.0 were processed in-house using WLUP procedures with NJOY2016.
- JEFF-3.1 and ENDF/B-VII.1 are directly obtained from the IAEA/WLUP Project [WLUP].

An extensive analysis and results of this exercise can be found at [UPM report: 2022-12-20/WP4-D4.6/R6]. This report summarizes the following results:

- Reactivity modification along the burnup (60 GWd/MTU) using full evaluations of nuclear data (neutron induced evaluation, thermal scattering, fission yield and decay data).
    - ENDF/B-VII.1 (E71) vs ENDF/B-VIII.0 (E80) and JEFF-3.3 (J33) for depletion.
    - ENDF/B-VII.1 is used as the reference or base library because it is the evaluation used in the industry for depletion calculations.
- Reactivity modification using the "same isotopes" predicted with ENDF/B-VII.1.
- Changes in main actinides.
- Changes in main fission products, assessing the impact of fission yields and decay data in reactivity

- Fission rates and neutron flux
    - Overestimation of ^{235}U fission collapsed cross-section in PWR-like spectrum?
    - Necessity of ND validation with reaction-rates in thermal systems…
  - Reactivity modification: JEFF-3.3 -> ENDF/B-VIII.0
    - ^{238}U
    - $^{238}U + ^{235}U$
    - $^{238}U + ^{235}U + ^{239}Pu$
    - $^{235}U + ^{238}U + ^{239}Pu$ + Fission Yields + Decay Data

An example of reactivity changes during burnup is presented in Figure 8 and Table 22. Figure 8 shows the modification of reactivity with the reference library ENDF/B-VII.1 versus ENDF/B-VIII.0 and JEFF-3.3 as a function of burnup. In Table 22, a comparison of reactivity with the reference library ENDF/B-VII.1 shows that both ENDF/B-VIII.0 and JEFF-3.3 significantly underestimate the reactivity at high burnup. However, this reactivity underestimation is reduced if we use the isotopic composition predicted with ENDF/B-VII.1. So, we may conclude that the transmutation buildup is playing an important role in the *"reactivity burnup issue"*.

Regarding this transmutation build-up, Figure 9 shows the modification of isotopic inventory for ^{239}Pu. This figure shows changes as a function of the burn-up . These changes can be attibutted to the effective microscopic cross-sections of mainly $^{238}U(n,\gamma)$ and ^{239}Pu(n,absortion) and the total neutron energy-integrated flux (calcualtions are performed at constant fission power).

In order to investigate the main contributors to these differences in reactivity, a substitution of different nuclear data is performed. Figure 10 shows the main contributors in k_{eff} for the JEFF-3.3 and ENDF/B-VII.1 comparison. In this case, ^{239}Pu, ^{238}U, fission yields + decay data (FY+DD) and ^{235}U are the main contributors. At 60 GWd/MTU, it can be seen that the FY+DD contribution is around -500pcm. However, this effect of FY+DD is not seen in ENDF/B-VIII.0 because FYs were taken over from ENDF/B-VII.1.

Additionally, this work includes an analysis of the impact of FY+DD in the isotopic inventory of some important fission products for reactivity: ^{135}I, ^{135}Xe, ^{103}Rh, ^{143}Nd, ^{145}Nd, ^{147}Sm, ^{149}Sm, ^{150}Sm, ^{153}Eu, ^{155}Gd, ^{152}Sm among others. An example of the impact of FYs can be seen in Figure 11. The Figure shows differences between a nuclear data library and ENDF/B-VII.1 in the ^{147}Sm concentration as a function of the burnup. It can be seen that a substitution of FYs in JEFF-3.3 by those FYS of ENDF/BVII.1 will significantly modify the ^{147}Sm concentration. The FYs/^{235}U for ^{147}Sm in ENDF/B-VII.1 is 0.0085794 while in JEFF-3.3 is 0.010552. Hence, these differences may explain the differences observed in Figure 11.

Table 21. Pin-cell Benchmark for burnup calculations

	Fuel	**Cladding**	**Moderator**
Temperature	873.0 K	608.52 K	583.0 K
Material	UO_2 (3.1% ^{235}U enrichment)	Zirconium	750 ppm Boron
Size (in cold conditions)	Outer-radius: 0.409575 cm	Outer-radius: 0.474980 cm	Pitch pin-cell: 1.259840 cm
POWERC – constant 36.22 MW/MTU			

Table 22. Reactivity changes (in pcm) in the pin-cell benchmark for different burnup steps.

	ENDF/B-VIII.0 - ENDF/B-VII.1		JEFF-3.3 - ENDF/B-VII.1	
	Nuclide composition with ENDF/B-VIII.0	Nuclide composition with ENDF/B-VII.1	Nuclide composition with JEFF-3.3	Nuclide composition with ENDF/B-VII.1
BOC No Xenon	-70	-70	+235	+235
BOC Xenon Eq.	-55	-2	+380	+325
60 GWd/MTU	-550	-65	-1500	-275

NOTE: BOC=Begin of Cycle

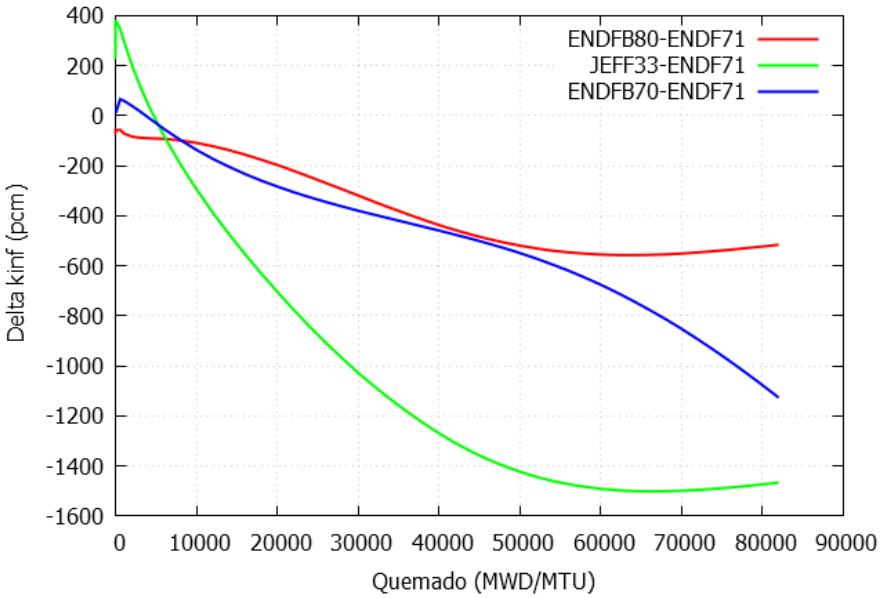

Figure 8. Reactivity modification at pin-cell level 3.1$^{w}/_{o}$ UO_2.

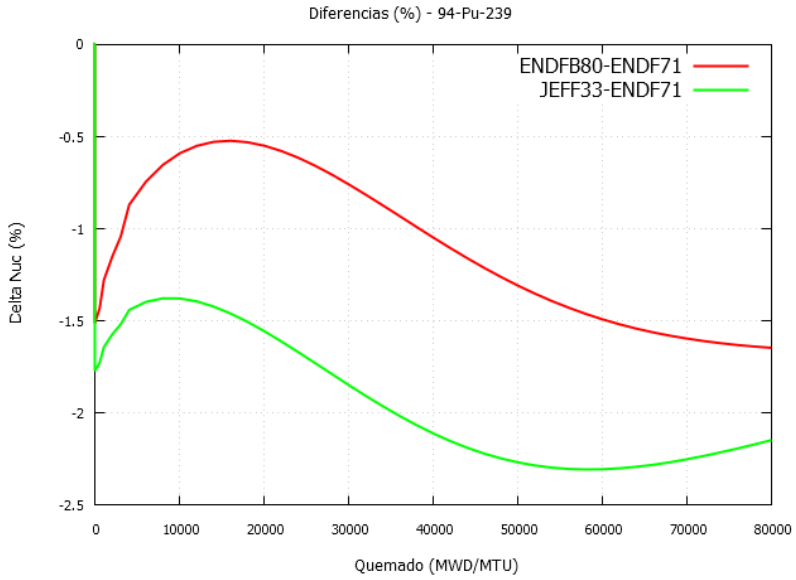

Figure 9. Nuclide modification: ^{239}Pu at pin-cell level 3.1$^{w}/_{o}$ UO_2.

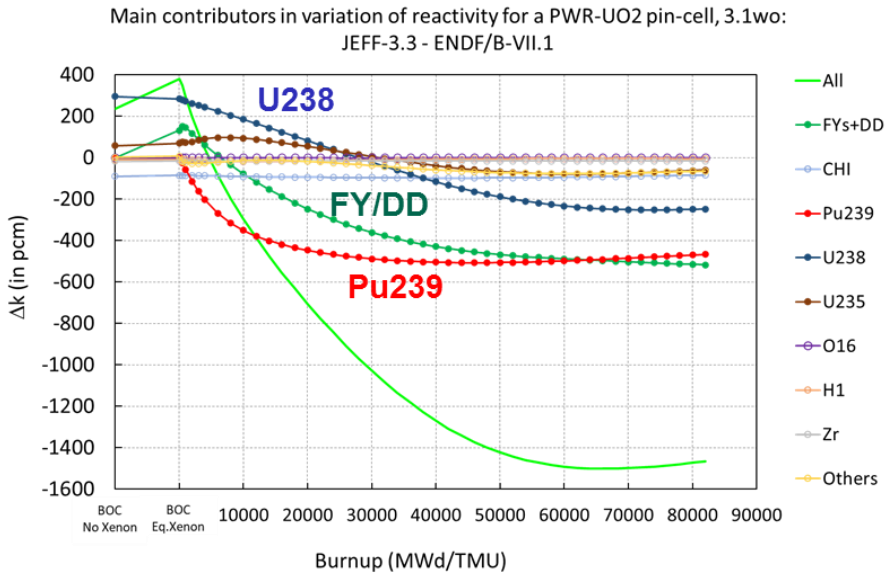

Figure 10. Reactivity modification at pin-cell level 3.1$^{w}/_{o}$ UO_2. Main contributors.

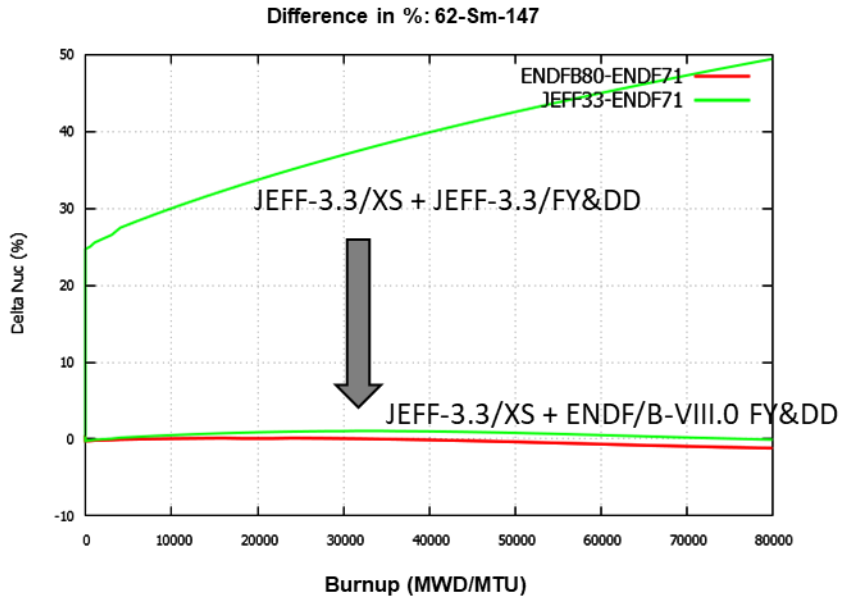

Figure 11. Nuclide ^{147}Sm modification as a function of fission yields and decay data.

5.5. Recommendations

Based on the overview of the SFCOMPO database and analyses performed with spent nuclear fuel, the following general recommendations can be given:

- Inclusion of decay heat data in the SFCOMPO database is strongly encouraged. These efforts are already underway within the framework of the OECD/NEA WPNCS SG12.
- Addition of measurements using NDA techniques in the SFCOMPO database is also strongly encouraged. Whereas some results of gamma-ray measurements are already included, especially neutron emission measurements have the potential to provide complementary insight and contribute to improved spent nuclear fuel characterisation.

- In many cases, a more detailed description of method of burnup determination and uncertainty assessment would be highly recommended or even required. Since the entire calculated nuclide vector depends on normalisation, this requirement would improve the accuracy and uncertainty assessment of all C/E comparisons.

Regarding the reactivity change with the burn-up, the main conclusions of the work performed can be summarized as follows:

- There is a need of a joint evaluation for depletion issues: ^{235}U-^{238}U-^{239}Pu … + fission yields / decay data. In particular, more work is needed on fission yields is needed to understand their impact in the reactivity. There is also a necessity of sensitivity coefficients which may depend on burnup and enrichment
- Simple burn-up calculations are very effective, and we have to introduce them in the nuclear data validation routine. A list of simple benchmarks should be defined that are representative of specific data and that can be checked by everybody with several codes. In particular, new JEFF-4Tbeta evaluations of ^{238}U should be tested in depletion calculations, because ^{238}U plays an important role in the build-up of ^{239}Pu.

5.6. References

[Carmouze 2021] C. Carmouze et al., *Synthesis of the subgroup 7 activities: Specification of a benchmark on Sensitivity / Uncertainty Analysis for PWR UOx spent nuclear fuel*. WPNCS Subgroup 7, OECD/NEA, Paris, 2021.

[CLAB 2006] Svensk Kärnbränslehantering AB (SKB), *Measurements of decay heat in spent nuclear fuel at the Swedish interim storage facility, Clab*. Report SKB Rapport R-05-62, 2006.

[Jansson 2022] P. Jansson, M. Bengtsson, U. Bäckström, F. Álvarez-Velarde, D. Čalič, S. Caruso, R. Dagan, L. Fiorito, L. Giot, K. Govers, A. Hernandez Solis, V. Hannstein, G. Ilas, M. Kromar, J. Leppänen, M. Mosconi, P. Ortego, R. Plukienė, A. Plukis, A. Ranta-Aho, D. Rochman, L. Ros, S. Sato, P. Schillebeeckx, A. Shama, T. Simeonov, A. Stankovskiy, H. Trellue, S. Vaccaro, V. Vallet, M. Verwerft, G. Žerovnik, A. Sjöland, *Blind Benchmark Exercise for Spent Nuclear Fuel Decay Heat*. Nucl. Sci. Eng. 196 (2022) 1125-1145. DOI: 10.1080/00295639.2022.2053489.

[JEFDOC-2111] O. Cabellos and A. Espaliú, *Comparison of Burnup Calculations for ND Validation Activities*, JEFF Nuclear Data Week, November 25, 2021, JEFDOC-2111 (in-person).

[JEFF/BU, 2021] O. Cabellos, *Pin-cell depletion Benchmark: ENDF/B-VII.0 - ENDF/B-VII.1, ENDF/B-VIII.0 and JEFF-3.3*, JEFF Burnup meeting, February 10, 2021.

[Leppänen 2013] J. Leppänen et al. *The Serpent Monte Carlo code: Status development an applications in 2013*. In Annals of Nuclear Energy 82 (2015) 142-150.

[Michel-Sendis 2017] F. Michel-Sendis, *SFCOMPO-2.0: An OECD NEA database of spent nuclear fuel isotopic assays, reactor design specifications, and operating data*. Ann. Nucl. Energy 110 (2017) 779-788. DOI: 10.1016/j.anucene.2017.07.022.

[Nureg 2006] I.C. Gauld *et al.*, *Validation of SCALE 5 Decay Heat Predictions for LWR Spent Nuclear Fuel*. Oak Ridge National Laboratory, 2006.

[Romojaro 2022] P. Romojaro, K. Ambrožič, D. Čalič, L. Fiorito, K. Govers, A. Hernandez-Solis, B. Kos, P. Schillebeeckx, A. Stankovskiy, G. Žerovnik and M. Kromar, *Sensitivity and uncertainty analysis of PWR spent fuel observables to operational and model parameters*. Proc. Int. Conf. PHYSOR 2022, p. 1854-1863.

[Schillebeeckx 2020] P. Schillebeeckx, M. Verwerft, G. Žerovnik, Y. Parthoens, B. Pedersen, G. Alaerts, G. Cools, K. Govers, J. Paepen, G. Varasano, R. Wynants, *A non-destructive method to determine the neutron production rate of a sample of spent nuclear fuel under standard controlled area conditions*. Report EUR 30379 EN, European Atomic Energy Community, Luxembourg, 2020.

[UPM report: 2022-12-20/WP4-D4.6/R7] O. Cabellos, *Study of different nuclear data libraries to predict reactivity change with burnup: "the burnup issue"*, UPM report: 2022-12-20/WP4-D4.6/R7

[Žerovnik 2018] G. Žerovnik *et al.*, *Observables of interest for the characterization of Spent Nuclear Fuel*, EUR 29301 EN, Publications Office of the European Union, Luxembourg, 2018, ISBN 978-92-79-90347-2, DOI: 10.2760/418524, PUBSY No JRC112361.

[WLUP] https://www-nds.iaea.org/wimsd/

6. Summary and conclusions

In this report we present a review of the state-of-the-art of benchmarking and validation of nuclear data. This includes both conventional criticality benchmarks and other type of benchmark experiments (shielding experiments, kinetic parameters, fuel depletion experiments). Some of the major points discussed in this document are:

- Even in the most conventional case of using criticality benchmarks (ICSBEP database) for validating nuclear data, it must be taken into account that validating a specific type of nuclear data requires and adequate selection of representative benchmarks with high sensitivity to the specific nuclear data. This involves using sensitivity values provided in some database and/or performing dedicated sensitivity calculations. Some general steps and criteria have been presented, alongside with some examples (123-Mosteller's suite, JEFF iron Working Group, selection of benchmarks for testing the unresolved resonance range and selection of LCT benchmarks for criticality safety analysis).
- Shielding benchmarks (SINBAD database) offer an alternative path for nuclear data validation. However, the SINBAD database is less developed than the ICSBEP database and should be used with more care. A considerable amount of work is being carried out to improve the quality of the SINBAD database.
- Regarding kinetic parameter (β_{eff} and Λ_{eff}) benchmarks, there is a limited number of data available in the IRPhE database, but additional experimental values can be found in other databases (ICSBEP) or the scientific literature. β_{eff} is highly sensitive to $\bar{\nu}_p$ and $\bar{\nu}_d$, while Λ_{eff} shows a high sensitivity to main fission-related data ((n,f), $\bar{\nu}$, $\bar{\nu}_p$) and, to a lower extent, to scattering cross sections of the main nuclides contributing to neutron moderation. The Rossi-α ($\alpha = -\beta_{eff}/\Lambda_{eff}$) is another parameter that can be also used for nuclear data validation, with the advantage of having experimental information available for more systems than from Λ_{eff}.
- Fuel depletion benchmarks, such as the ones included in the SFCOMPO database, represent an additional path for nuclear data validation, being particularly useful for data such as fission yields or the ^{238}U(n,γ) and ^{239}Pu(n,absortion) cross sections. Proposed improvements include the inclusion of decay heat data, a better characterization of spent fuel through non-destructive techniques (e.g. neutron emission measurements) and a more detailed description of the fuel burn-up history.

7. Acknowledgements

The ICSBEP, IRPhE, SINBAD and SFCOMPO databases have been obtained through the NEA Computer Program Services. The MCNP code has been obtained through Radiation Safety Information Computational Center (RSICC).

In addition to the SANDA project, a part of the work has been funded by the RCUK Energy Programme [grant number EP/T012250/1]. To obtain further information on the data and models underlying this paper please contact PublicationsManager@ukaea.uk.

Annex 1. List of SINBAD fission, fusion and accelerator shielding benchmarks

Table 23. Fission Shielding Experiments in SINBAD. Benchmarks with quality review include notes. Codes in brackets mean that inputs are available, but not yet included in the database.

Benchmark	Shielding material	Detectors	Computer code input
ASPIS Iron (♦♦)	Fe 1.2m	Au, Rh, In, S foils, NE213 scintillator	DOT3.5
ASPIS Iron 88 (♦♦♦)	steel 67 cm	Au, Rh, In, S, Al foils	MCBEND, DORT, TORT, MCNPX/-5, (SERPENT)
ASPIS Graphite (♦♦♦)	graphite 0.7 m	Rh, In, S, Al foils	DOT3.5, MCNPX/-5
ASPIS PCA REPLICA (♦♦♦)	H_2O /Fe shield	Mn, Rh, In, S, ^{235}U foils, SP-2, NE213 scintillator	DOT3.5,TORT, TRIPOLI-3, -4, MCNPX/-5/-6.1
ASPIS Water (♦♦♦)	H_2O 50 cm	S foils, NE213 scintillator	TRIPOLI, MCNPX/-5
ASPIS n-gamma Transport (♦♦♦)	H_2O /steel arrays	Rh, S, Mn foils, TLD, ionization chamber	MCNPX /-5
NESDIP-2 (ASPIS) (♦/♦♦)	H_2O /stainless steel (SS)	S, In, Rh foils	MCNPX /-5
NESDIP-3 (ASPIS) (♦♦♦)	PWR radial shield, cavity	Rh, S foils, H proportional counters, NE213 scintillator	MCBEND, MCNPX/-5
JANUS Phase I (♦♦♦)	mild & stainless steel	Mn, Au, Rh, S foils, H proportional counters, NE213 scintillator	MCBEND, MCNPX/-5
JANUS Phase VIII (♦♦♦)	mild steel and Na	Mn, Au, Rh, S foils	MCNPX /-5
Ispra Na (EURACOS) (♦♦)	Na 360 cm	S, Au foils, H proportional counters	MCNP3
Ispra Fe (EURACOS) (♦♦)	Fe 130 cm	S, In, Rh, Au foils, NE213, gas proportional counters	MCNP3, MCNP4C
Cadarache Sodium (HARMONIE) (♦)	Na	Rh, S, Na, Mn, Au foils, SP2 proton recoil spectra (relative measurements)	ANISN, DOT3.5
Karlsruhe Iron Sphere	Fe 15-40 cm	proton recoil, He-3 spectrometers	None
Wuerenlingen Iron (PROTEUS)	Fe, stainless steel 80 cm	Rh, In, S foils, SP2 proton recoil spectra	None
Neutron Leakage from Water Spheres (NIST)	H_2O	fission chambers ($^{235,238}U$, ^{237}NP, ^{239}Pu)	MCNP
Streaming Through Ducts (IRI-TUB)	Ducts (air)	Fe, Ni, In, Mn, Au, Sc foils, TLD	DOT3.5
Gamma Production Cross Sections from Thermal Neutron Capture	Fe, SS, N, Na, Al, Cu, Ti, Ca, K, Cl, Si, Ni, Zn, Ba, S	NaI (Tl) crystal	None
Gamma-ray Production Cross Sections from Fast Neutron Capture	Fe, O, Al, Cu, Zi, Ti, K, Ca, S, Si, Ni, Ba, S, stainless steel	NaI (Tl) crystal	None
JASPER Advanced Reactor Axial Shield	stainless steel, B_4C	Bonner balls, NE213 scintillator, proton-recoil counters, Hornyak button detector	None

Table 24. Fission Shielding Experiments in SINBAD (cont.)

Benchmark	Shielding material	Detectors	Computer code input
JASPER Advanced Reactor Intermediate Heat Exchanger	Na	Bonner balls, NE213 scintillator, proton-recoil counters	None
JASPER Advanced Reactor Radial Shield	stainless steel, graphite, B_4C, boral, Na	Bonner balls, NE213 scintillator, proton-recoil counters	None
ORNL TSF Iron Broomstick	Fe	NE213	None
ORNL TSF Oxygen Broomstick	O	NE213 scintillator	None
ORNL TSF Nitrogen Broomstick	N	NE213 scintillator	None
ORNL TSF Sodium Broomstick	Na	NE213 scintillator	None
ORNL TSF Stainless Steel Broomstick	4-inch-diameter oxygen	NE213 scintillator	None
ORNL Neutron Transport Through Fe & SS - Part I	iron and stainless steel	NE213 scintillator	None
ORNL Neutron Transport in Thick Na	Na	NE213 scintillator	None
Pool Critical Assembly-Pressure Vessel Facility	core-to-cavity region in a LWR	Np, U, Rh, In, Ni, Al foils	None
University of Illinois Iron Sphere (CF-252)	shell of iron	NE213 scintillator	None
University of Tokyo-YAYOI Iron Slab	iron slabs, up to 20-cm-thick	NE213 scintillator, spherical proportional detectors of H_2 and CH_4 gas	None
PV monitoring in NRI LR-0 VVER-440	VVER-440 pressure vessel neutron dosimetry	Neutron spectra by proton recoil	None
PV monitoring in NRI LR-0 VVER-1000	VVER-1000 PV neutron dosimetry	Neutron–gamma spectra using scintillation spectrometer	None
Balakovo-3 VVER-1000	VVER-1000 ex-vessel neutron dosimetry	Np, U, Nb, Ni, Fe, Ti, Cu, Nb foils	DORT
VENUS-3 LWR-PVS (♦♦♦)	3 loop Westinghouse LWR pressure vessel	Ni, In, Al foils	MCNP4B, TORT, DORT
H.B. Robinson-2 Pressure Vessel	3 loop LWR in-/ex-vessel n dosimetry	Cu, Ti, Fe, Ni, U, Np foils	DORT, MCNP
RFNC Photon Leakage Spectra	Al, Ti, Fe, Cu, Zr, Pb, ^{238}U spheres	stilbene scintillation	MCNP5
RFNC Photon Spectra from H_2O, SiO_2 and NaCl	H_2O, SiO_2 and NaCl	stilbene scintillation	MCNP5
IPPE Th shell with 14 MeV & ^{252}Cf neut. (♦♦♦)	Th shell r=13 cm	fast scintillator	MCNP4C
IPPE Bi shell with 14 MeV & ^{252}Cf neut (♦♦♦)	Bi shells r=12 cm	fast scintillator	MCNP4C

Table 25. Fission Shielding Experiments in SINBAD (cont.)

Benchmark	Shielding material	Detectors	Computer code input
Baikal-1 Skyshine Benchmark (♦♦♦)	Heavy serpentinite concrete, 1.1-1.4 m thick; steel	several spectrometers	MCNP
NAÏADE 1 Graphite Benchmark	Graphite (60cm)	^{32}S(n,p), ^{103}Rh(n,n'), ^{31}P(n,p), silicon diodes, ^{55}Mn(n,γ), ^{197}Au(n,γ), ^{115}In(n,γ)	TRIPOLI
NAÏADE 1 Iron Benchmark	Fe (60cm)	^{31}P(n,p), silicon diodes, ^{103}Rh(n,n'), ^{55}Mn(n,γ), ^{115}In(n,γ), ^{197}Au(n,γ), fission chambers (^{237}Np, ^{235}U & ^{239}Pu)	TRIPOLI
NAÏADE 1 Light Water Benchmark	H_2O (60cm)	^{31}P(n,p), ^{103}Rh(n,n'), silicon diodes, ^{32}S(n,p), photomultiplier, ^{115}In(n,γ), ^{197}Au(n,γ), BF_3 counters, ^{55}Mn(n,γ)	TRIPOLI
NAÏADE 1 Concrete Benchmark	Concrete (60cm)	^{31}P(n,p), ^{103}Rh(n,n'), silicon diodes, ^{115}In(n,γ), ^{197}Au(n,γ), ^{55}Mn(n,γ)	TRIPOLI
Photon Skyshine Benchmark	air	gamma spectra by ionization chamber	None
SNL Polyethylene Reflected Pu Metal Sphere- Subcritical Neutron and Gamma Measurements	stainless steel 304	• gross neutron counter • neutron multiplicity counter • high-resolution gamma spectrometer	None

Table 26. Fusion neutronics shielding experiments in SINBAD. Notes are included for quality reviewed compilations. Codes in brackets mean that inputs available, but yet to be included.

Benchmark	Shielding material	Detectors	Computer code input
OKTAVIAN Ni Sphere (♦♦♦)	Ni sphere r=16 cm	NE213 scintillator (TOF)	MCNP5, (SuperMC)
OKTAVIAN Fe Sphere (♦♦)	Fe sphere r=50.32 cm	TOF: NE213 scintillator, Li-6 glass scintillator	MCNP5, (SuperMC)
OKTAVIAN Al Sphere (~♦♦♦)	Al - 10 cm	NE218 scintillator (TOF), NaI crystal	MCNP5, (SuperMC)
OKTAVIAN W Sphere (~♦♦♦)	W – 10 cm	NE218 scintillator (TOF), NaI crystal	MCNP5, (SuperMC)
OKTAVIAN Si Sphere (~♦♦♦/♦♦)	Si – 20 and 30 cm	NE218 scintillator (TOF), NaI crystal	MCNP5, (SuperMC)
OKTAVIAN Mn Sphere (~♦♦♦)	Mn – 60 cm	NE218 scintillator (TOF)	MCNP5 (X) (SuperMC)
FNS Graphite Cylindrical Assembly (~♦♦♦)	graphite 31.4 cm x 61.0 cm	fission chambers (^{235}U,^{238}U,^{232}Th, ^{237}Np), fission track detectors, Al, Ni, Zr, Nb, In, Au foils, NE213, TLD	DOT3.5, MCNP5, (SuperMC)
FNS Liquid Oxygen (♦♦♦)	liquid O 20 cm	NE213 scintillator (TOF)	DOT3.5, MCNP5, (SuperMC)
FNS Vanadium Cube (~♦♦♦)	V cube 25.4 x 25.4 x 25.4 cm^3	NE213, proton recoil counters (PRC), BF_3 counter, Al, Nb, In, Au foils, BC537, TLD	MCNP5, (SuperMC)
FNS Tungsten (~♦♦♦)	W (2r=62.9 cm, h= 50.7 cm)	NE213, PRC, BF_3 counter, Al, Nb, In, W, Au foils, BC537, TLD	MCNP5, (SuperMC)
FNS Skyshine (♦♦)		rem-counters, ^{3}He, BF_3, Ge detectors, NaI crystal	MCNP5, (SuperMC)
FNS Dogleg Duct Streaming (♦♦/♦♦♦)	iron slab 170 cm x 140 cm x 180 cm	NE213 scintillator; Nb, In, Au foils,	MCNP5, (SuperMC)
FNS fusion neutronics (1983-1991)	Li, Pb-Li, Pb-Li-C, Be-Li, Be-Li-C, Li_2O	NE213 scintillator; foils	DOT3.5, MCNP5
FNG-SS Shield (integral) (~♦♦♦)	stainless steel 60 cm	Al, Fe, Ni, In, Mn, Au foils	MCNP5, DORT, (SuperMC)
FNG-ITER Blanket Bulk Shield (integral) (♦♦♦)	ITER inboard shield	Al, Fe. Ni, Nb, In, Mn, Au foils, TLD-300	MCNP5, DORT, (SuperMC)
FNG/TUD ITER Blanket Bulk Shield (spectra) (~♦♦♦)	ITER inboard shield	NE213 scintillator	MCNP5
FNG-ITER Neutron Streaming (integral) (♦♦♦)	ITER shielding system	Nb, Al, Ni, Au foils, TLD-300	MCNP5, DORT
FNG-ITER Dose Rate Experiment (♦♦♦)	stainless steel/ H_2O assembly	Ni foils, TLD-300	MCNP5
FNG Silicon Carbide (integral) (♦♦♦)	SiC (45.72 x 45.72 x 71.12cm^3)	Au, Al, Nb, Ni foils, TLD	MCNP5, DORT, TWODANT

Table 27. Fusion neutronics shielding experiments in SINBAD (cont.)

Benchmark	Shielding material	Detectors	Computer code input
FNG/TUD Silicon Carbide (spectra) (~♦♦♦)	SiC (45.72 x 45.72 x 71.12cm^3)	NE213 scintillator	MCNP5
FNG Tungsten (integral) (♦♦♦)	W block 42-47 x 46.85 x 49 cm^3	Au, Mn, In, Ni, Fe, Al, Zr, Nb foils TLD	MCNP5, DORT, TWODANT
FNG HCPB Tritium Breeder Module (♦♦♦)	metallic Be with 2 layers of Li_2CO_3	Au, Ni, Al and Nb foils, Li_2CO_3 pellets (T breeding), TLD-300	MCNP5, DORT-TORT
FNG/TUD W (spectra) (~♦♦♦)	W block 42-47 x 46.85 x 49 cm3	NE213 scintillator	MCNP5
TUD Iron Slab Experiment (~♦♦♦)	iron slab 30 cm	NE213 scintillator	MCNP5
IPPE Vanadium Shells (~♦♦♦)	V spheres r=5 & 12 cm	fast scintillator	MCNP4C
IPPE Iron Shells (♦♦♦)	Fe spheres r=4.5-30 cm	fast scintillator	MCNP4C
ORNL 14-MeV Neutron SS/ Borated Poly Slab	stainless steel	NE213 scintillator	None
University of Illinois Iron Sphere (D-T)	Fe sphere r=38.1cm	NE213 scintillator	None
KANT Spherical Beryllium Shells	Be shells 5, 10, 17 cm thick	NE213, Bonner sphere	MCNP
MEPhI empty slits streaming exp.	Fe shielding with empty slits	In, Zn, Al, Fe, F, ^{233}U foils, TLD, stilbene crystals	MCNP4C2
Juelich Li Metal Blanket	stainless steel	Li_2CO_3 samples in Al sample holders, TLD detectors and activation foils	MCNP

Table 28. Accelerator Shielding Experiments in SINBAD (benchmarks with quality review include notes).

Benchmark	Shielding material	Projectile	Detectors	Computer code input
Transmission of n & γ Generated by 52 MeV p (♦♦)	C (< 64.5 cm thick), Fe (< 57.9 cm), H_2O (< 101 cm), concrete (<115 cm)	52 MeV protons on C target	NE213 scintillator	MCNPX
Transmission of n & γ generated by 65MeV p	concrete, Fe, Pb, graphite (10-100 cm thick)	65 MeV protons on Cu target	NE213 scintillator	None
AVF75-Transmission of Medium Energy Neutrons Through Concrete Shields (1991) (♦♦)[1]	concrete	75-MeV proton beam incident on a stopping-range Cu assembly	7.6-cm-diameter x 7.6-cm-long NE-213 scintillator	MCNPX[1]
Neutron Production from Thick Targets of C, Fe, Cu, Pb by 30 & 52-MeV Protons (1982)	stainless steel 316	30- and 52-MeV protons incident on C, Fe, Cu, and Pb targets	NE 213 scintillator	MCNPX
TIARA 40 and 65 MeV Neutron Transmission (♦♦♦)[1]	Fe (130 cm), concrete (< 200 cm), polyethylene (< 180cm)	43 and 68 MeV protons on Li-7 target	BC501A, Bonner ball, fission counters, TLD, SSNTD	MORSE-CG, HETC-KFA2, DORT, MCNP4B, LAHET, (more MCNP to be included)
Radioactivity Induced by GeV-Protons &Spallation Neutrons (2001)	B, C, Al, Fe, Cu, Nb, HgO, Pb, Pb, acrylic resin, SS-316, Inconel	2.83 and 24 GeV protons on mercury target	HPGe	None
Intermediate and High-Energy Accelerator Shielding Benchmarks	C, Al, and Fe	113 and 800 MeV protons	BC-418 plastic scintillators	None
ROESTI I, II and III	Fe and Pb (100 cm thick)	200 GeV/c hadrons (2/3 p^+,1/3 π^+) (Roesti I&III), 24 GeV/c p^+ (Roesti II)	In, S, Al, C foils, RPL	FLUKA92
CERF Bonner Sphere response to charged hadrons	polyethylene/Cd/Pb	120 GeV/c positive hadrons(1/3 p and 2/3 π)	Bonner sphere - a SP9 3He counter	FLUKA
CERF Radionuclide Production (~2003)	steel, Cu, Ti, concrete, light materials (e.g. C composites, B- nitride)	120 GeV/c mixed hadrons (1/3 p, 2/3 π^+)	Germanium (HPGe) for gammas	FLUKA
CERF Residual Dose Rates (2003)	Al, Cu, Fe, Ti, concrete	120 GeV/c mixed hadrons (1/3 p , 2/3 π^+)	NaI crystal	FLUKA
CERF shielding experiment at CERN (2004)	cylindrical Cu target	120 GeV/c mixed hadron (1/3 p, 2/3 π^+)	NE213 organic liquid scintillator	MARS15

[1] Quality evaluation performed under NEA contract, available to be included in SINBAD.

Table 29. Accelerator Shielding Experiments in SINBAD (cont.)

Benchmark	Shielding material	Projectile	Detectors	Computer code input
CERN 200 and 400 GeV/c protons activation experiments (1983)	Cu targets	200 GeV/c and 400 GeV/c extracted protons	Thermo-, photo-luminescent & optical absorption glass dosimeters, Al, Au, S, Cu foils & plastic scintill.	None
RIKEN Quasi-monoenergetic Neutron Field (70-210 MeV)	air	70 – 210 MeV protons on ^{7}Li	NE213 scintillator (TOF)	None / EXFOR reference
KENS p-500 MeV shielding experiment at KEK	concrete	500MeV protons on thick W target	Activation of Bi, Al, In and Au foils	MARS14
HIMAC He, C, Ne, Ar, Fe, Xe and Si ions on C, Al, Cu and Pb targets (♦♦♦)	C, Al, Cu and Pb targets	100-800 MeV/ nuc. He, C, Ne, Ar, Fe, Xe & Si ions	NE213 & NE102A scintillators	MCNPX
HIMAC/NIRS High Energy Neutron (up to 800 MeV) (♦♦)	Fe (up to 100 cm)	400 MeV/nucleon C ions on Cu target	Neutron spectra by Self-TOF, NE213	MCNPX
HIMAC/NIRS High Energy Neutrons (< 800 MeV) (♦♦)	Concrete (up to 250 cm)	400 MeV/nucleon C ions on Cu target	Self-TOF, NE213, Bi and C foils	MCNPX
BEVALAC Experiment - Nb Ions on Nb & Al Targets (♦♦♦)[1]	Nb (0.51 and 1 cm thick) and Al (1.27 cm thick)	272 & 435 MeV/nucl. Nb ions	NE-102 scintillator	MCNPX[1]
MSU 155 MeV/ nucleon He & C ions on Al target (♦♦♦)	Al (13.34 cm)	155 MeV/nucleon He and C ions	BC-501, NE213 (TOF)	MCNPX
PSI - High Energy Neutron Spectra Generated by 590-MeV Protons on Pb Target (♦/♦♦)[1]	Pb target (60 cm)	590 MeV protons	NE213 (TOF)	MCNPX[1]
ISIS Deep Penetration of Neutrons through Concrete & Fe (♦♦♦)	Concrete (120 cm) and Fe (60 cm)	800 MeV protons on Ta target	C, Bi, Al, In_2O_3 foils, n & γ dosimeters	MCNPX
TEPC-FLUKA Comparison for Aircraft Dose (♦/♦♦)	Air	^{60}Co (γ), 0.5 MeV n source, AmBe source, CERN/ CERF (120 GeV p & π on Cu)	TEPC	None

[1] Quality evaluation performed under NEA contract, available to be included in SINBAD.

Classification used:

♦ ♦ ♦	Valid for nuclear data and code benchmarking
♦ ♦	Benchmarks of intermediate quality, suitable for education and training
♦	Benchmarks of historical interest

Annex 2. List of SINBAD benchmarks with quality review completed

Table 30. SINBAD fission benchmarks with quality review completed (17 in total). Main domains requiring further attention and additional information needed are listed.

Benchmark	Improvement	Additional information needed on
ASPIS Iron ~ ♦♦		neutron source description, positioning / dimension uncertainty, some specifications inconsistent or not complete
ASPIS Iron-88 ~ ♦♦♦ [1]	New MCNP model added.	Missing information on detectors arrangement (e.g. stacking), gaps between the slabs and effect of the cave walls
ASPIS Graphite ♦♦♦	New MCNP model added.	Additional information needed such as detector arrangement in the slots (some dimensions are inconsistent)
ASPIS Water ♦♦♦	New MCNP model added.	Supplementary information needed on NE-213 spectrometer, water tank dimensions (container, bowing effects) and experimental room
ASPIS n/γ water/steel arrays ~ ♦♦♦	New MCNP model added.	Supplementary information needed on detectors arrangement, bowing of the water tanks, background subtraction and cave walls effect
ASPIS PCA REPLICA ♦♦♦	As above	Supplementary information needed on set-up of the activation foils and rear wall of the ASPIS cave
NESDIP-2 ♦ / ♦♦	- new MCNP model	- activation foils positioning & housing - background subtraction method
NESDIP-3 ♦♦♦ [1]	- new detailed MCNP model	- activation foils positioning & housing - background subtraction method
JANUS-1 ♦♦♦	- new detailed MCNP model	- activation foils positioning & housing - background subtraction method
JANUS-8 ♦♦♦	- new detailed MCNP model	- activation foils positioning & housing - background subtraction method
EURACOS Iron ~ ♦♦ [1]	New MCNP5 model, source model and uncertainty added.	source (spectrum, spatial distribution), energy structure of the proton recoil spectra, neutron spectrometers response functions, additional details on the geometry (room return), on geometry and material composition uncertainties. Limited applicability – fast neutron attenuation in iron only.
EURACOS Na ~ ♦♦ [1]	- same as above -	- same as above -
HARMONIE ♦	/	too simplified description of geometry, materials and neutron source
VENUS-3 ♦♦♦		Data 1st released to SINBAD, detailed evaluation done in ICSBEP
BAIKAL-1 ♦♦♦		Data 1st released to SINBAD, detailed evaluation done in ICSBEP
IPPE Th shell with 14 MeV & 252Cf neutron source ~ ♦♦♦		More details on collimator duct and detector needed, experimental bare ^{252}Cf source spectra not available
IPPE Bi shell with 14 MeV & ^{252}Cf neutron source ~♦♦♦		More details on collimator and detector housing needed, bare ^{252}Cf source spectra not available

Table 31. SINBAD fusion neutronics benchmarks with quality review completed (25 in total). Main domains requiring further attention and additional information needed are listed.

Benchmark	Improvement	Additional information needed on
OKTAVIAN W n/γ spec. ~ ♦♦♦	- new routine & detailed MCNP model - benchmark data evaluation	- background subtraction method - γ source measurements - γ detector response function
OKTAVIAN Al ~ ♦♦♦	- new routine & detailed MCNP model - benchmark data evaluation	- neutron flight path parameter - background subtraction method - γ source measurements & γ detector response function
OKTAVIAN Fe ~ ♦♦♦ or ♦♦	- new routine MCNP model	- very large measurement uncertainties
OKTAVIAN Si 60cm ~ ♦♦♦,	- new routine & detailed MCNP model - benchmark data evaluation	- background subtraction method - γ source measurements & detector response function
OKTAVIAN Si 40cm ♦♦	- new routine & detailed MCNP model	- neutron flux measurements only available in graphical form
OKTAVIAN Ni ♦♦♦	- new routine MCNP model	
OKTAVIAN Mn ♦♦♦	- new routine MCNP model	supplementary information would be needed on background subtraction method and gamma source measurements
FNG SiC ♦♦♦	- neutron source re-evaluation	/
FNG/TUD SiC ~ ♦♦♦	- re-evaluation of benchmark source term	- neutron & γ flux point–wise uncertainties - original pulse-height distributions - inconsistencies with FNG-SiC benchmark results
TUD Iron slab ~ ♦♦♦	- new routine MCNP model	Supplementary information needed on neutron source and pulse height spectrum
FNG Stainless Steel ~ ♦♦♦	- neutron source re-evaluation	- a comprehensive geometry description would be helpful
FNG ITER Dose Rate ♦♦♦	- neutron source re-evaluation	/
FNG/TUD ITER Bulk Shield ~ ♦♦♦	- neutron source re-evaluation	- neutron and gamma flux point–wise uncertainties - original pulse-height distributions
FNG ITER Neutron streaming ♦♦♦	- neutron source re-evaluation	/
FNG W ♦♦♦	re-evaluation of benchmark source term	/
FNG/TUD W ~ ♦♦♦	re-evaluation of benchmark source term	- neutron & γ flux point–wise uncertainties - measured pulse-height distributions - inconsistencies with FNG–W bench.results
FNG HCPB ♦♦♦		
FNS Graphite ~ ♦♦♦	- new detailed MCNP model	- experimental unfolding technique, - activation foils positioning & housing

Table 32. SINBAD fusion neutronics benchmarks with quality review completed (cont.)

Benchmark	Improvement	Additional information needed on
FNS V ~ ♦♦♦	- new detailed MCNP model - benchmark data evaluation	- experimental unfolding technique - activation foils positioning, uncertainty & housing
FNS W ~ ♦♦♦	- new detailed MCNP model - benchmark data evaluation	- unfolding technique of NE–213 measurements - activation foils positioning, uncertainty & housing
FNS Iron dogleg-duct ♦♦	/	- neutron source spectrum - neutron detector response function
FNS Oxygen ♦♦♦		- neutron effective flight path parameter
FNS Sky-shine ♦♦		- neutron source spectrum
IPPE-V shells, 14 MeV n source ~ ♦♦♦	New 2D & 3D MCNP5 models prepared	- collimator duct
IPPE-Fe shells, 14 MeV n source ♦♦♦	New 2D & 3D MCNP5 models prepared	- collimator duct
IPPE-Th shell with 14 MeV & ^{252}Cf neutron source	2D&3D MCNP5 models prepared	more details on collimator and detector needed, experimental bare ^{252}Cf source spectra not available,
IPPE-Bi shells with 14 MeV & ^{252}Cf neutron source		collimator and detector housing needed, bare ^{252}Cf source spectra not available
MSU 155 MeV/nucleon He & C ions on Al targets	MCNPX model prepared	/ experiments are adequate for benchmarking of calculation models and codes
Tokyo Uni. transmission through C, Fe, H2O & concrete of n/□ generated by 52MeV protons	MCNPX model prepared	experimental information should be recovered; experimental uncertainty needed on: proton energy, density, H content in concrete, unfolding process
ISIS 800 MeV protons (120cm Concrete & 60cm Iron)	MCNPX model prepared	/ experiment is adequate for benchmarking purposes
HIMAC 400 MeV/ nucleon C ions on concrete shield	PHITS model prepared	reduction in unfolding uncertainty, estimate of experimental uncertainty should be obtained before these experiments could be used for benchmarking processes
HIMAC 400 MeV nucleon C ions on Fe shield	PHITS model prepared	large measurement uncertainties, unfolding uncertainty and parameter uncertainties needed,
HIMAC 100-800 MeV/nucleon heavy ions	MCNPX model prepared	/ experiments are adequate for benchmarking purposes

Table 33. SINBAD accelerator benchmarks with quality review completed (10 in total). Main domains requiring further attention and additional information needed are listed.

Benchmark	Improvement	Additional information needed on
MSU 155 MeV /nucleon He & C ions on Al targets (♦♦♦)	MCNPX model prepared	/ experiments are adequate for benchmarking of calculation models and codes
Tokyo Uni. transmission of 52 MeV protons through C, Fe, H_2O & concrete (♦♦)	MCNPX model prepared	experimental information should be recovered; experimental uncertainty needed on: proton energy, density, H content in concrete, unfolding process
ISIS 800 MeV protons (120 cm Concrete & 60 cm Iron) (♦♦♦)	MCNPX model prepared	/ experiment is adequate for benchmarking purposes
HIMAC 400 MeV/nucl. C ions on concrete shield (♦♦)	PHITS model prepared	reduction in unfolding uncertainty, estimate of experimental uncertainty should be obtained before these experiments could be used for benchmarking processes
HIMAC 400 MeV/ nucleon C ions on Fe shield (♦♦)	PHITS model prepared	large measurement uncertainties, unfolding uncertainty and parameter uncertainties needed,
HIMAC 100-800 MeV /nucleon heavy ions (♦♦♦)	MCNPX model prepared	/ experiments are adequate for benchmarking purposes
AVF75-Transmission of Medium Energy Neutrons Through Concrete Shields (1991) (♦♦)[1]	New MCNPX model prepared	Shortcomings: - complete lack of uncertainty information on the measured data - lack of information about the collimator geometry and materials - large uncertainty in results for 50 and 100cm concrete.
TIARA 40 and 65 MeV Neutron Transmission (♦♦♦)[1]	New MCNPX models prepared	New review underway.
BEVALAC Experiment - Nb Ions on Nb & Al Targets (♦♦♦)[1]	New MCNPX models prepared.	
PSI - High Energy Neutron Spectra Generated by 590-MeV Protons on Pb Target (♦/♦♦)[1]	New MCNPX models prepared	Found inadequate for the benchmarking due to complete lack of uncertainty information on the measured data.

Annex 3. Complete list of kinetics benchmarks

NOTE: sensitivity profiles computed with the techniques described in section 4 are available at http://www.sanda-nd.eu/D4.6_sensitivity_profile_data_files for the systems with the following labels:

❶	Sensitivity profiles for β_{eff}
❷	Sensitivity profiles for Λ_{eff}

Table 34. Summary of ^{235}U benchmark systems *with* kinetic information.

System	ICSBEP/IRPhE name	β_{eff} (pcm)	Λ (s)	α (s^{-1})	References
Godiva ❶ LANL 1950s 94% U_{MET} sphere No reflector	HEU-MET-FAST-001	659 ± 10	---	---	[Meulekamp 2006] [Leppänen 2014]
Orsphere ❶ ❷ ORNL 1970s 93% U_{MET} sphere No reflector	HEU-MET-FAST-100 ORSPHERE-FUND-EXP-001	657 ± 9[1]	5.94 (± 0.08) × 10^{-9}	-1.1061 (± 0.0009) × 10^{6}	ICSBEP, p. 32 IRPhE, p. 28-33
Topsy ❶ ❷ LANL 1964-66 93% U_{MET} sphere Natural U_{MET} reflector	HEU-MET-FAST-028	665 ± 13[2]	1.74 (± 0.03) × 10^{-8}	-38.2 × 10^{4}	[Meulekamp 2006] [Leppänen 2014] [ANL 6681] p.14
Coral ❶ CIEMAT 1973 90% U_{MET} cylinder Natural U_{MET} reflector	HEU-MET-FAST-062	663 ± 17	---	---	[De Francisco 1973]
ZPR-9/34 (ZPR-HEU) ❶ ANL 1979 93% ^{235}U fuel. Reflected by SS	HEU-MET-INTER-001	667 ± 2%	---	---	[ANL-81-72] p. 7 [Leppänen 2014]
ZPR-3/23 ANL 1959 93% U_{MET}/Al fuel Reflected by DU	HEU-MET-FAST-055	---	---	-5.63 (± 2%) × 10^{4}	[ANL 6681] p.14
ZPR-9/4 ANL 1964 93% U_{MET} + W core Al reflector	HEU-MET-FAST-060	---	---	-5.19 (± 5%) × 10^{4}	[ANL 7007] p.34
ZPR-9/6 ANL 1959 93% U_{MET}/Al fuel Reflected by DU	HEU-MET-FAST-067	---	---	-4.67 (± 0.31) × 10^{4}	[ANL 7208] p. 99

[1] β_{eff} = 657 ± 2 pcm is reported in IRPhE and 657 ± 9 in ICSBEP. A lower value of β_{eff} = 602 ± 8 pcm is reported in [Mihalczo 1976], but it is considered wrong in IRPHE's documentation.

[2] The values listed in [ANL 6681] p.14 are β_{eff} = 690 pcm and Λ = 1.82 × 10^{-8} s. The value of Λ = 1.74 × 10^{-8} s has been calculated considering β_{eff} = 665 pcm.

Table 35. Summary of ^{235}U benchmark systems with kinetic information (cont.)

System	ICSBEP/IRPhE name	β_{eff} (pcm)	Λ (s)	α (s^{-1})	References
ZPR-9/7 ANL 1959 93% U_{MET}/Al fuel Reflected by DU	HEU-MET-FAST-070	---	---	-1.51 (± 0.95) $\times 10^3$	[ANL 7208] p. 99
ZPR-9/8 ANL 1959 93% U_{MET}/W/Al/Al_2O_3 core Al/Al_2O_3/Be/BeO reflector	HEU-MET-FAST-070	---	---	-1.27 (± 0.27) $\times 10^3$	[ANL 7208] p. 99
FCA-XIX-1 ❶ JAEA 1996-98 94% ^{235}U /C core (depl.) UO_2/Na reflector	---	742 ± 24	---	---	[Okajima 2002] [Leppänen 2014] [Kodeli 2017]
MASURCA R2 ❶ CEA 1993-94 75% ^{235}U fuel (depl.) UO_2/Na reflector	---	721 ± 11	---	---	[Okajima 2002] [Leppänen 2014] [Kodeli 2017]
Big Ten ❶ LANL 1971 10% ^{235}U fuel (depl.) U reflector	IEU-MET-FAST-007	720 ± 7	---	---	[Meulekamp 2006] [Leppänen 2014] [Kodeli 2017]
ZPR-6/9 (ZPR-U9) ❶ ANL 1980-81 9% ^{235}U fuel DU reflector	IEU-MET-FAST-010	725 ± 2%	---	---	[ANL-81-72] p. 7 [Leppänen 2014]
ZPR-3/41 ANL 1962 16% U_{MET}/Al/SS core DU reflector	IEU-MET-FAST-012	---	---	-5.55 (± 3%) $\times 10^4$	[ANL 6681] p.14
ZPR-9/1 ANL 1964 ~11% U_{MET} core Al reflector	IEU-MET-FAST-013	---	---	-8.67 (± 5%) $\times 10^4$	[ANL 7007] p.34
ZPR-9/2 ANL 1964 ~16% U_{MET} + W core Al reflector	IEU-MET-FAST-014	---	---	-6.9 (± 5%) $\times 10^4$	[ANL 7007] p.34
ZPR-9/3 ANL 1964 ~21% U_{MET} + W core Al reflector	IEU-MET-FAST-014	---	---	-6.57 (± 5%) $\times 10^4$	[ANL 7007] p.34
ZPR-3/6F ANL 1957 47% U/Al/SS core DU reflector	IEU-MET-FAST-015	---	---	-9.4 (± 3%) $\times 10^4$	[ANL 6681] p.14

Table 36. Summary of ^{235}U benchmark systems with kinetic information (cont.)

System	ICSBEP/IRPhE name	β_{eff} (pcm)	Λ (s)	α (s^{-1})	References
ZPR-3/11 ANL 1958 ~12% U core DU reflector	IEU-MET-FAST-016	---	---	-10.3 (± 3%) $\times 10^4$	[ANL 6681] p.14
ZPR-6/6A ANL 1969-70 DU/Na/FeO/depl. U_3O_8 /93% $^{235}U_{MET}$ core DU reflector	IEU-COMP-FAST-001	---	---	-10.0 (± 5%) $\times 10^4$	[ANL 7007] p. 34
FR0-3X ❶ Studsvik 1964-71 20% U_{MET}/C core Copper reflector	IEU-MET-FAST-022	719[3] ± 16 774 ± 17	---	---	ICSBEP, p. 57 [Kockum 1970] Table 2, p. 13 [Moberg 1972] Table 7, p. 17 [Moberg 1973] Table II, p. 348
FR0-5 ❶❷ Studsvik 1964-71 20% $U_{MET}/CH_2/C/Al$ core Copper reflector	IEU-MET-FAST-022	735[4] ± 18 752 ± 18	2.84[5] (± 0.03) $\times 10^{-7}$	---	
FR0-8 ❶ Studsvik 1964-71 20% U_{MET}/CH_2/C core Copper reflector	IEU-MET-FAST-022	735[6] ± 16 780 ± 17	---	---	
BFS1-73 ❶ IPPE (Russia) 1997 18.5% U_{MET}/Na core Depl. UO_2 reflector	BFS1-LMFR-EXP-001	720[7] ± 27 740 ± 15	---	---	IRPhE, p. 40 [Kodeli 2017]
TCA 1.83U[8] ❶ JAEA (Japan) 1964 2.6% UO_2 fuel rods Water moderator	LEU-COMP-THERM-006	771 ± 19	---	---	[Nakajima 2001] [Meulekamp 2006] [Leppänen 2014]
MB-01 ❶❷ IPEN 2014-16 4.35% UO_2 fuel rods Water moderator	LEU-COMP-THERM-077 IPEN(MB01)-LWR-RESR-001	750 ± 19	31.96 (± 1.06) $\times 10^{-6}$	---	IRPhE, p. 228-229

[3] Upper value from [Moberg 1972] and lower value from [Moberg 1973].
[4] Upper value from [Moberg 1972] and lower value from [Moberg 1973].
[5] Taken from [Kockum 1970] table 2, p. 13. Measured in a slightly subcritical configuration. Rossi-α values also listed, but all correspond to subcritical configurations.
[6] Upper value from [Moberg 1972] and lower value from [Moberg 1973].
[7] Upper value was measured with the ^{252}Cf source technique and lower value was measured with the Rossi-α technique. A weighted average value of 735 ± 13 is recommended.
[8] β_{eff} measurement described in [Nakajima 2001] was performed in a variant of the 1.83U lattice described in the benchmark (cases 4 to 8) with a cylindrical instead of square arrangement of fuel rods.

Table 37. Summary of ^{235}U benchmark systems with kinetic information (cont.)

System	ICSBEP/IRPhE name	β_{eff} (pcm)	Λ (s)	α (s^{-1})	References
Winco Slab Tanks[9] LANL 1989 93.1% uranyl nitrate sol. No reflector	HEU-SOL-THERM-038	1500[10] ± 12% 1450 ± 13%	---	-1109.3 ± 0.3% -1152.7 ± 1.2%	[Spriggs 1993] [Meulekamp 2006] [Leppänen 2014]
Stacy run 29 JAEA 1995 10% uranyl nitrate sol. Water reflector	LEU-SOL-THERM-004	---	---	-122.7 ± 4.1	[Tonoike 2002] [Meulekamp 2006] [Leppänen 2014]
Stacy run 30 JAEA 1995 10% uranyl nitrate sol. Water reflector	LEU-SOL-THERM-004	---	---	-126.8 ± 2.9	[Tonoike 2002] [Meulekamp 2006] [Leppänen 2014]
Stacy run 33 JAEA 1995 10% uranyl nitrate sol. Water reflector	LEU-SOL-THERM-004	---	---	-116.7 ± 3.9	[Tonoike 2002] [Meulekamp 2006] [Leppänen 2014]
Stacy run 46 JAEA 1995 10% uranyl nitrate sol. Water reflector	LEU-SOL-THERM-004	---	---	-106.2 ± 3.7	[Tonoike 2002] [Meulekamp 2006] [Leppänen 2014]
Stacy run 125 JAEA 1997 10% uranyl nitrate sol. Water reflector	LEU-SOL-THERM-016	---	---	-152.8 ± 2.6	[Tonoike 2002] [Meulekamp 2006] [Leppänen 2014]
Stacy run 215 JAEA 1998 10% uranyl nitrate sol. No reflector	LEU-SOL-THERM-021	---	---	-109.2 ± 1.8	[Tonoike 2002] [Meulekamp 2006] [Leppänen 2014]

[9] In [Meulekamp 2006] it is stated that the measurements correspond to Case 5 in the benchmark, we consider it to correspond more likely to Case 1 (no absorber/reflector). Nevertheless, in [Spriggs 1993] it is stated that the critical separation between uranyl tanks was ~9.9 cm, while in the benchmark's documentation it is listed as 9.38 cm for Case 1 and 9.27cm for Case 5.

[10] Upper values for β_{eff} and α were obtained with a single ^{3}He detector and lower values were obtained with a combination of four ^{3}He detectors in the assembly midplane. Experimental values for β_{eff} seem too large; in [Spriggs 1993] inaccuracies in "*the measurement of the intrinsic source strength of the fuel*" are given as a possible explanation.

Table 38. Summary of Pu and mixed fuel benchmark systems with kinetic information.

System	ICSBEP/IRPhE name	β_{eff} (pcm)	Λ (s)	α (s^{-1})	References
Jezebel ❶ LANL 1950s Pu sphere No reflector	PU-MET-FAST-001	194 ± 10	---	---	[Meulekamp 2006] [Leppänen 2014] [Kodeli 2017]
Popsy ❶❷ LANL 1960s Pu sphere Natural U_{MET} reflector	PU-MET-FAST-006	276 ± 7	1.21 ± 0.03 $\times 10^{-8}$	-22.9 $\times 10^{4}$	[ANL 6681] p.14 [Meulekamp 2006] [Leppänen 2014] [Kodeli 2017]
ZPR-6/10 (ZPR-Pu) ❶ ANL 1981-82 Pu/C/SS core SS/Fe reflector	PU-MET-INTER-002	221.7 ± 2%	---	---	[ANL-81-72] p. 7
ZPR-3/59 ❶ ANL 1969 Pu/C core Pb reflector	PU-MET-INTER-004	233 ± 10	---	---	[Carpenter 1972]
ZPR-9/31 (ZPR-MOX) ❶ ANL 1976-77 (Pu, U)C core Depl. UC reflector	MIX-COMP-FAST-005	381 ± 2%	---	---	[ANL-81-72] p. 7 [Leppänen 2014]
SNEAK-7A ❶ KIT 1970-71 MOX fuel Graphite reflector	SNEAK-LMFR-EXP-001	395 ± 4%	---	---	IRPhE p. 36 [Fischer 1977] [Leppänen 2014] [Kodeli 2017]
SNEAK-7B ❶ KIT 1970-71 MOX fuel Natural UO_2 reflector	SNEAK-LMFR-EXP-001	429 ± 4%	---	---	IRPhE p. 36 [Fischer 1977] [Leppänen 2014] [Kodeli 2017]
MASURCA Zona2 ❶ CEA 1993 MOX/Na core (depl.) UO_2/Na reflector	---	349 ± 6	---	---	[Okajima 2002] [Leppänen 2014] [Kodeli 2017]
FCA XIX-2 ❶ JAEA 1996/98 Pu/NU/Na core (depl.) UO_2/Na reflector	---	364 ± 9	---	---	[Sakurai 1999] [Okajima 2002] [Leppänen 2014] [Kodeli 2017]
FCA XIX-3 ❶ JAEA 1996/98 Pu core (depl.) UO_2/Na reflector	---	251 ± 4	---	---	[Sakurai 1999] [Okajima 2002] [Leppänen 2014] [Kodeli 2017]

Table 39. Summary of ^{233}U benchmark systems with kinetic information.

System	ICSBEP/IRPhE name	β_{eff} (pcm)	Λ (s)	α (s^{-1})	References
Skidoo ❶ LANL 1961 ^{233}U sphere No reflector	U233-MET-FAST-001	290 ± 10	---	---	[Meulekamp 2006] [Leppänen 2014] [Kodeli 2017]
Flattop 23 ❶❷ LANL 1964 ^{233}U sphere Natural U_{MET} reflector	U233-MET-FAST-006	360 ± 14[11]	1.33 (± 0.05) × 10^{-8}	-2.71 × 10^{5}	ICSBEP p. 6 [Meulekamp 2006] [Leppänen 2014] [ANL 6681] p.14 [Kodeli 2017]

References

[ANL 6681] G. S. Brunson *et al.*, *A survey of prompt-neutron lifetimes in fast critical systems*. ANL-6681 (1963).

[ANL 7007] R. C. Doerner *et al.*, *Physics measurements in tungsten-based aluminium-reflected fast reactors*. ANL-7007 (1967).

[ANL 7208] R. C. Doerner *et al.*, *ZPR-9 assemblies no. 6-9 critical experiments*. ANL-7208 (1967).

[ANL-81-72] E. F. Bennett, *An experimental method for reactor-noise measurements of effective beta*. ANL-81-72 (1981).

[Carpenter 1972] S. G. Carpenter *et al.*, *Measurements of the Effective Delayed-Neutron Fraction in Two Fast Critical Experiments*. Nuclear Science and Engineering 49 (1972) 236-239.

[De Francisco 1973] J. L. de Francisco *et al.*, *Determinación de la fracción efectiva de neutrones retardados en el Reactor CORAL-I*, J.E.N report No. 275.

[Fischer 1977] E. A. Fischer, *Integral Measurements of the Effective Delayed Neutron Fractions in the Fast Critical Assembly SNEAK*, Nuclear Science and Engineering 62 (1977) 105-106.

[Kockum 1970] J. Kockum, *Analysis of Pulsed Source Experiments Performed in Cooper-Reflected Fast Assemblies*. Atomenergi report AE-399, 1970.

[Kodeli 2017] I. Kodeli *et al.*, *Uncertainty Analysis of Kinetic Parameters for Design, Operation and Safety Analysis of SFRs*, Proc. Int. Conf. on Fast Reactors and Related Fuel Cycles: Next Generation Nuclear Systems for Sustainable Development (FR17), Yekaterinburg (Russian Federation) 26-29 June 2017.

[Leppänen 2014] J. Leppänen et al., *Calculation of effective point kinetics parameters in the Serpent 2 Monte Carlo code*. Annals of Nuclear Energy 65 (2014) 272-279.

[Meulekamp 2006] R. K. Meulekamp and S. C. van der Marck, *Calculating the Effective Delayed Neutron Fraction with Monte Carlo*. Nuclear Science and Enginnering 152 (2006) 142-148.

[Mihalczo 1976] J. T. Mihalczo, *The Effective Delayed Neutron Fraction from Fission in an Unreflected Uranium Sphere from Time Correlation Measurements with Californium-252*. Nuclear Science and Engineering 60 (1976) 262-275.

[Moberg 1972] L. Moberg and J. Kockum, *Measurement of the Effective Delayed Neutron Fraction in Three Different FR0-cores*. Atomenergi report AE-456, 1972.

[11] In [Meulekamp 2006] and [Leppänen 2014], an uncertainty is listed as ±9. Also, in [ANL 6681] p.14 the values listed are β_{eff} = 355 pcm and, correspondingly, $\Lambda = 1.31 \times 10^{-8}$ s.

[Moberg 1973] L. Moberg and J. Kockum, *Measurement of the Effective Delayed Neutron Fraction in Three Different Cores of the Fast Assembly FR0*. Nuclear Science and Engineering 52 (1973) 343-349.

[Nakajima 2001] K. Nakajima, *Re-evaluation of the Effective Delayed Neutron Fraction Measured by the Substitution Technique for a Light Water Moderated Low-enriched Uranium Core*, Journal of Nuclear Science and Technology 38 (2001) 1120-1125.

[Okajima 2002] S. Okajima *et al.*, *Summary on international benchmark experiments for effective delayed neutron fraction (β_{eff})*. Progress in Nuclear Energy 41 (2002) 285-301.

[Sakurai 1999] T. Sakurai *et al*., *Experimental Cores for Benchmark Experiments of Effective Delayed Neutron Fraction (β_{eff}) at FCA*. Progress in Nuclear Energy 35 (1999) 131-156.

[Spriggs 1993] G. D. Spriggs, *A Measurement of the Effective Delayed Neutron Fraction of the Westinghouse Idaho Nuclear Company Slab Tank Assembly Using Rossi-α Techniques*. Nuclear Science and Engineering 115 (1993) 76-80.

[Tonoike 2002] K. Tonoike *et al.*, *Kinetic Parameter β_{eff}/l Measurement on Low Enriched Uranyl Nitrate Solution with Single Unit Cores (600φ, 280T, 800φ) of STACY*. Journal of Nuclear Science and Technology 39 (2002) 1227-1236.

Annex 4. Number of burnable absorber rods vs. initial enrichment in BWR CLAB 2006 cases.